Palaeogeography, Palaeoclimatology, Palaeoecology 634 (2024) 111914

Contents lists available at ScienceDirect

Palaeogeography, Palaeoclimatology, Palaeoecology

journal homepage: www.elsevier.com/locate/palaeo

# Barnacle-rich facies as a tool for palaeoenvironmental reconstructions

Giovanni Coletti [a,*], Giulia Bosio [a], Alberto Collareta [b], Or Mordecai Bialik [c,d], Eleonora Regattieri [e], Irene Cornacchia [e], Gianni Insacco [f], John Buckeridge [g]

[a] Dipartimento di Scienze dell'Ambiente e della Terra, Università di Milano-Bicocca, Piazza della Scienza 4, 20126 Milano, Italy
[b] Dipartimento di Scienze della Terra, Università di Pisa, Via Santa Maria 53, 56126 Pisa, Italy
[c] Institute of Geology and Paleontology, University of Münster, Corrensstr. 24, 48149 Münster, Germany
[d] Dr. Moses Strauss Department of Marine Geosciences, The Leon H. Charney School of Marine Sciences, University of Haifa, Carmel 31905, Israel
[e] Istituto di Geoscienze e Georisorse, Consiglio Nazionale delle Ricerche, Via G. Moruzzi 1, 56124 Pisa, Italy
[f] Museo Civico di Storia Naturale di Comiso, Via degli Studi 9, 97013 Comiso, Italy
[g] Earth & Oceanic Systems Group, RMIT University, GPO Box 2476, VIC 3001, Melbourne, Australia

ARTICLE INFO

Editor: Professor L Angiolini

*Keywords:*
Pliocene
Pleistocene
*Chelonibia*
*Concavus*
*Perforatus*
Stable isotope geochemistry

ABSTRACT

Palaeoenvironmental data are fundamental in determining the manifold impacts of climate change. This paper argues that sessile barnacles are an excellent palaeoenvironmental proxy: they are present in nearly all nearshore environments, and their shell consists of diagenetically stable low-magnesium calcite and grows fast enough to record short-term variations. To demonstrate their utility, specimens from several Western Mediterranean Pliocene and Pleistocene barnacle-rich deposits are analysed herein, using for the first time a combination of sedimentology, taphonomy, stable isotope geochemistry and detailed comparisons with modern counterparts. Within shelf carbonate systems, barnacle diversity is highest in the shallow, nearshore waters and decreases moving offshore, thus providing a good proxy for the reconstruction of water depth and distance from the coastline. Barnacle taphonomy is also informative. Well-preserved complete specimens are characteristic of protected areas, whereas less well-preserved specimens occur in high-energy areas. The presence/absence of opercular plates is also particularly relevant for evaluating hydrodynamic conditions. As regards the C and O stable isotope ratios, due to the porous and coarse-grained nature of the deposits in which barnacle remains are usually found, the shells are often exposed to meteoric water percolation during diagenesis. Among the analysed specimens, only those collected from fine-grained deposits display no evidence of alteration and have isotopic ratios in line with those of their modern counterparts. These fossils display intra-shell variations that in modern barnacles have been related to short-term environmental changes (e.g., seasonal cycles). These results demonstrate that barnacles can always be useful for detailed palaeoenvironmental reconstructions based on skeletal assemblages. Furthermore, with further research aimed at gathering more data and assessing potentially interfering signals, they could become useful proxies for palaeoseasonality.

## 1. Introduction

To address the challenges posed by global warming, a fundamental goal for geology is the provision of reliable information on the Earth's past environmental conditions. The Pliocene-Pleistocene represents a key interval, with broad environmental variations that may be regarded as a useful analogue of what we may need to endure in the near future (e.g., Crowley and Hyde, 2008; Lunt et al., 2008; Haywood et al., 2013; Hill et al., 2014; Prista et al., 2015). Our knowledge of these variations is essentially based on the analysis of deep-sea sediments (e.g., Shackleton et al., 1984; Raymo et al., 1997; Bartoli et al., 2005; Bailey et al., 2013). Non-turbiditic, deep-sea sedimentation mostly consists of a slow and relatively constant fall-out of fine-grained sedimentary particles, generally resulting in a continuous – albeit condensed and thus poorly resolved – record of environmental variations. Sedimentation rates in shallow-water are generally higher – thus theoretically allowing for a better resolution of short-term variability – but the record is usually more discontinuous (e.g., Ager, 1973), thus reducing the potential for high-resolution reconstructions. As proxies for determining past environments in shallow-water contexts, barnacles display four key

* Corresponding author.
*E-mail address:* giovanni.coletti@unimib.it (G. Coletti).

https://doi.org/10.1016/j.palaeo.2023.111914
Received 10 May 2023; Received in revised form 5 November 2023; Accepted 12 November 2023
Available online 18 November 2023

advantages, related to their wide distribution in marine systems, abundance, shell mineralogy and growth rates, respectively. Barnacle shells are made of low-magnesium calcite (Clarke and Wheeler, 1922; Chave, 1954; Bourget, 1974; Smith et al., 1988; Hover et al., 2001; Borromeo et al., 2017; Collareta et al., 2018; Ullmann et al., 2018), which is more stable and less soluble than both aragonite and high-Mg calcite. Barnacle shells grow relatively quickly (Crisp and Bourget, 1985, and references therein; López et al., 2012) and may thus record short-term environmental oscillations such as seasonal variability (Buckeridge, 1975; Killingley and Newman, 1982). Furthermore, thanks to their high growth rate, barnacles can rapidly accumulate conspicuous shells (Hoskin and Reed, 1984; Buckeridge, 1999, 2015; Coletti et al., 2018b, and references therein), thus resulting in faithful palaeontological "snaphots" of past environments. On these grounds, barnacles and barnacle-rich facies represent powerful instruments for performing detailed palaeonvironmental reconstructions. Thus, the aim of this work is to explore the environmental signal recorded by barnacles during the geological past and provide guidelines for their use in future research. Several Pliocene-Pleistocene barnacle-rich deposits of northwestern and central Italy (Fig. 1) are studied herein, and a palaeoenvironmental analysis is provided for each site by focusing on the sedimentology, barnacle abundance in the skeletal assemblage, and barnacle taphonomy. Then, the C and O stable isotope ratios of barnacle shells are investigated, testing different settings (very shallow, shallow, and intermediate depth), time-intervals (Early Pliocene, mid-Pliocene, Late Pliocene, and Early Pleistocene), types of barnacles (both epizoic and non-epizoic forms), and types of embedding deposits (fine-grained and coarse-grained sediments).

## 2. Barnacle shell geochemistry

Calcareous barnacles form their shell as a succession of thin calcite layers deposited about an organic matrix (Bourget, 1987; Gal et al., 2015). These layers consist of calcite crystals enveloped in organic macromolecules and display hierarchical patterns related to seasonal and ontogenetic changes in the growth rate (Bourget and Crisp, 1975; Gal et al., 2015). Although this structure is appealing for geochemical analyses (Burgess et al., 2010), only a few investigations have been carried out on this invertebrate group. Most of the studies on modern barnacles have been concerned with their attachment to various surfaces due to the negative economic impact of barnacle fouling (e.g., Christie and Dalley, 1987; Swain et al., 1998). Other analyses have been focused on trace element abundances to evaluate the possibility of using barnacles as biotracers of pollution (Walker and Foster, 1979; Watson et al., 1995; Hockett et al., 1997; Darmoian and Al-Marsoumi, 2002; Türkmen et al., 2005; Reis et al., 2011). Element/Ca ratios of barnacle shells have been studied and proposed as tracers of salinity (Gordon et al., 1970) and elevation from the shore level (Pilkey and Harris, 1966; Bourget, 1974). However, detailed analyses have shown that elemental ratios, such as the Ca/Mg ratio, are strongly associated with the shell's organic content, indicating the affinity of these elements with the organic matrix rather than with the calcite lattice of the shell (Barnes et al., 1976). Significant local effects have also been reported (Albuquerque et al., 2016). Overall, the chemical composition of barnacle shells is currently poorly understood; compilations of barnacle shell chemistry rely on very few samples, with the little available data indicating that barnacle shells are quite different from those of most other marine invertebrates (Carpenter and Lohmann, 1992; Khalifa et al., 2011; Iglikowska et al., 2018; Ullmann et al., 2018).

The C and O stable isotope ratios composition of modern barnacles have also been investigated for ecological and environmental purposes. The $\delta^{13}C$ and $\delta^{18}O$ values of sessile barnacles are sensitive to seasonal temperature variations, and the oxygen-isotope ratio has been proposed as a palaeothermometer (Killingley and Newman, 1982; Smith et al., 1988). C and O stable isotope ratios in epizoic barnacles (i.e., those that preferentially live over other marine organisms; e.g., Seilacher, 2005) have been employed to trace the movement patterns of their host animals (Killingley, 1980; Killingley and Lutcavage, 1983; Newman and Killingley, 1985; Detjen et al., 2015; Pearson et al., 2019, 2020). Achituv et al. (1997) investigated the $\delta^{13}C$ in extant Red Sea barnacles, suggesting its potential use as a tracker of barnacle food sources, while Craven et al. (2008) highlighted its potential as palaeoindicator of the elevation from the shore level. While the works of Burgess et al. (2010), Bojar et al. (2018) and Ullmann et al. (2018) have suggested that cirripede shells develop in isotopic equilibrium with the surrounding seawater, Killingley and Newman (1982) recorded that the calcite of recent balanomorph barnacle shells display systematically higher $\delta^{18}O$ values than expected at equilibrium. Overall, the paucity of studies investigating the C and O stable isotope composition of barnacle shells do not provide conclusive evidence in this regard. Even less data are

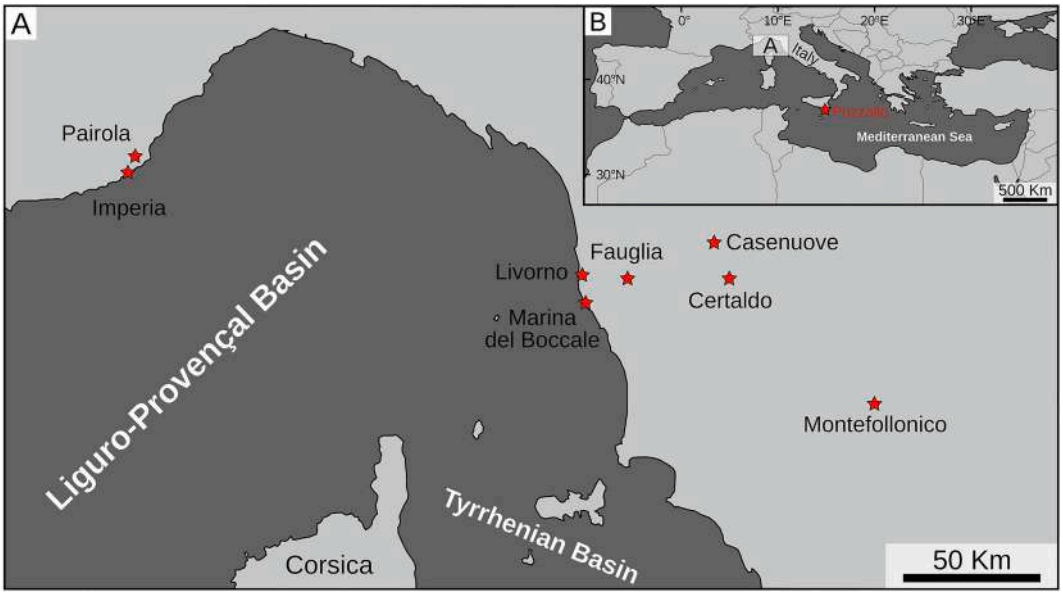


**Fig. 1.** Study area. A) Location of the studied Pliocene and Pleistocene outcrops and sampling sites of modern barnacles in the Western Mediterranean area. B) Position of the study area within the Mediterranean region and location of the sampling site of the investigated modern specimens of *Chelonibia testudinaria* (Pozzallo).

available on the stable isotope ratios of fossil barnacle shells. To our knowledge, very few studies have investigated the geochemical features of extinct cirripedes (e.g., Buckeridge, 1975; Gale and Schweigert, 2016; Bosio et al., 2020; Paces et al., 2023), and even less have focused on their O and C stable isotope ratios, namely, those by Roskowski et al. (2010), Collareta et al. (2018) and Taylor et al. (2019, 2022).

## 3. Geological setting

The Mediterranean region is dominated by the convergence between the African and European plates, a scenario that is further complicated by the presence of several smaller plates in-between. This convergence created the "alpide" orogenic belts (including the Alps and Apennines) as well as the many (sub)basins that comprise the present-day Mediterranean Sea, such as the Ligurian-Provençal Basin (which originated in late Oligocene to Early Miocene times) and the Tyrrhenian Basin (which originated in the Miocene) (Van Dijk and Scheepers, 1995; Carminati et al., 1998; Doglioni et al., 1999; Gelabert et al., 2002; Faccenna et al., 2007; Savelli, 2015; Loreto et al., 2021).

Coupled with the uplift of the Alpine External Massif, the subsidence of the Ligurian–Provençal Basin led to the formation of the late Neogene Ligurian coastal basins (Boni et al., 1976; Giammarino, 1984; Breda et al., 2007, 2009), while the eastward migration of the Apennine subduction resulted in the opening of the 'neoautochtonous' basins of Tuscany (Doglioni et al., 1999; Bizzarri and Baldanza, 2020; Brogi, 2020). During the Pliocene, the western Ligurian coast was bordered to the north by the rising Alpine massif and to the south by the subsiding Ligurian–Provençal Basin (Fanucci et al., 1980; Giammarino, 1984; Breda et al., 2007, 2009). Uplift started in the Late Miocene and peaked during the early Piacenzian (~3.5 Ma) (Boni et al., 1976; Giammarino, 1984; Bigot-Cormier et al., 2000; Giammarino and Piazza, 2000; Foeken et al., 2003). The resulting coastline was characterised by a very narrow continental shelf, a steep slope (Fanucci et al., 1980; Rehault et al., 1984, 1985), and several basins and sub-basins with a comb-like orientation with respect to the coastline (Boni et al., 1976). The 'neoautochtonous' basins of Tuscany started to form on the Tyrrhenian margin of the Northern Apennines during the Miocene and progressively developed eastward, following the migration of the subduction front (Martini and Sagri, 1993). This resulted in the development of various sets of basins parallel to the rising Apennines and bordered seawards by fringes of topographic highs. These basins can be distinguished into 'central' and 'peripheral' ones, with the former containing marine as well as Miocene deposits, versus the quintessentially Pliocene-Pleistocene continental fill of the peripheral basins (Martini and Sagri, 1993). The present work focuses on the central basins, which are geographically located west of the Cetona–Chianti Ridge (Fig. 1).

### 3.1. The Lower Pliocene Pairola succession

Within the Pliocene coastal basins of Western Liguria, three main formations (hereinafter: Fms) can be recognised: the Brecce di Taggia, the Argille di Ortovero and the Conglomerati di Monte Villa (Giammarino et al., 2010; Dalla Giovanna et al., 2016). Located in the western part of Liguria, the investigated outcrop at Pairola (43.94°N; 8.09°E; Fig. 1) consists of very coarse-grained, lithoclastic to bioclastic rudites that pass upwards into bioclastic calcarenites and finally into marls (Boni et al., 1976; Dalla Giovanna et al., 2016; Coletti et al., 2021a). The basal portion of the Pairola succession, belonging to the Conglomerati di Monte Villa Fm, hosts an abundant fossil assemblage dominated by barnacle fragments. The upper part of the Pairola succession, ascribed to the Argille di Ortovero Fm, is dominated by foraminifera (Boni et al., 1976; Dalla Giovanna et al., 2016; Coletti et al., 2021a). Based on planktic foraminiferal biostratigraphy (Boni et al., 1976), the Pairola succession spans between the MPL1 (corresponding to 5.3–5.1 Ma, Violanti, 2012) and the upper part of MPL4b (3.3–3.2 Ma, Violanti, 2012), with barnacle-rich layers being limited to the early–middle Zanclean (Coletti et al., 2021a). These layers have been interpreted as having formed in a narrow, high-energy, coastal environment, at a water depth of <30 m (Coletti et al., 2021a).

### 3.2. The mid-Pliocene Certaldo succession

The Certaldo outcrop (43.56°N; 11.03°E; Fig. 1) is located within the Valdelsa Basin of central Tuscany. Measuring *c.* 60 × 25 km, this NW-trending basin is filled with some 1000 m of continental-to-marine, uppermost Miocene to lowermost Pleistocene deposits (Benvenuti et al., 2014). The succession exposed at Certaldo consists of massive mudstones belonging to the Argille Azzurre Fm. An intraformational unconformity divides the Argille Azzurre strata of the Valdelsa Basin into a lower and an upper part ("lower" and "upper" blue clays), dated to the basal Zanclean and to the Zanclean–Piacenzian boundary, respectively (Benvenuti et al., 2014). The succession exposed at Certaldo belongs to the "upper blue clays" and has been referred to the S3 Synthem of Benvenuti et al. (2014). This large-scale sequence is mostly represented by an alternation of deltaic sands and mudstones overlain by shelf mudstones, which in the study area include several shell beds (Dominici et al., 2018). At the Certaldo outcrop, one of such horizons is exposed; it is rich in molluscs (mostly bivalves and gastropods) and barnacles, and also features cartilaginous fish remains (Collareta et al., 2020, 2021a,b). Based on their faunal assemblage and sedimentological characteristics, these deposits have been interpreted as the results of sedimentation in an off-shore setting at a depths of a few tens of meters (Benvenuti et al., 2014; Dominici et al., 2018). According to Benvenuti et al. (2014), the planktic foraminiferal assemblages from the S3 mudstones indicate the MPL 4 zone, corresponding to 3.98–3.19 Ma. Calcareous nannofossil assemblages from the same strata are indicative of the CNPL 4 zone, whose bounding bioevents have been calibrated to 3.82 and 2.76 Ma (Benvenuti et al., 2014). In light of these considerations, the investigated deposits cropping out at Certaldo are referred to the 3.82–3.19 Ma interval (late Zanclean – early Piacenzian).

### 3.3. The Upper Pliocene Casenuove succession

The Casenuove outcrop (43.69°N; 10.95°E; Fig. 1) is located at the northern edge of the Valdelsa Basin, near Empoli. The sedimentary succession exposed at this site has been referred by Dominici et al. (2018) to the mid-Piacenzian (*c.* 3 Ma) and belongs to the S5 Synthem of Benvenuti et al. (2014). This synthem displays a maximum thickness of about 200 m and consists of several smaller-scale sequences. Each sequence is tens of meters thick and comprises fluvial/coastal, coarse-grained sediments as well as open shelf mudstone, either topped by regressive shoreface/deltaic sandstones or directly overlain by the following sequence (Dominici et al., 2018). At Casenuove, four terrigenous marine sequences are exposed, forming a transgressive trend (Dominici et al., 1995). Within these strata, abundant plates of *Chelonibia testudinaria* (Linnaeus, 1758) were collected from around a balaenid (right whale) skeleton, the likely host organism of these epizoic cirripedes (Bianucci, 1996; Collareta et al., 2016; Collareta, 2020). The horizon embedding these fossils is part of the highstand deposits occurring near the top of the third depositional sequence and is characterised by abundant molluscan remains, including *Cerastoderma edule* (Linnaeus, 1758). The presence of this extant bivalve species suggests a very-shallow (approximately 10 m or less; Símonarson, 1981) setting, most likely corresponding to an interdistributary bay (Dominici et al., 1995).

### 3.4. The Upper Pliocene Montefollonico succession

The Montefollonico outcrop (43.13°N; 11.73°E; Fig. 1) belongs to the Siena-Radicofani Basin, a NNW-trending tectonic depression that provides one of the best records of post-collisional deposition in the hinterland of the Northern Apennines (Martini et al., 2021). Past authors

have often supported the identification of two distinct basins, the northern Siena Basin and the southern Radicofani Basin, but modern studies have highlighted a shared geological evolution (Brogi, 2011; Brogi et al., 2014). At the study site, a relatively inconspicuous carbonate unit occurs at the top and along the northwestern flank of an isolated hill, resting disconformably upon older, Lower Pliocene deposits (Nalin et al., 2016). Conglomerates are found at the base of the succession. Moving up-section, fossiliferous fine-grained calcirudites form most of the outcrop, being particularly rich in barnacles and coralline algae (Nalin et al., 2016). The lack of tractive structures, the poor sorting and the high matrix content suggest a relatively low-energy hydrodynamic setting (Nalin et al., 2016), which is consistent with a partly sheltered coast as documented elsewhere in the Siena-Radicofani Basin (Martini and Aldinucci, 2017). Due to the lack of biostratigraphic data, the chronostratigraphic assignment of these strata is somewhat ambiguous. In fact, these deposits could be alternatively correlated with subchrons C2An.1n, C2An.2n or C2An.3n (Nalin et al., 2016). Consequently, they are here conservatively regarded as Late Pliocene (Piacenzian) in age.

### 3.5. The Lower Pleistocene Fauglia succession

The Fauglia quarry (43.56°N; 10.53°E; Fig. 1) is located in the northern sector of the Tora-Fine Basin, one of the most external Neogene extensional basins of Tuscany (Bossio et al., 1999). During the Early Pleistocene, a changing tectonic regime induced the fragmentation of the Tora-Fine Basin, and the Fauglia area became a site of marine deposition (Bossio et al., 1999) (Fig. 1A). In the study area, the Pleistocene succession overlies Pliocene deposits (Marroni et al., 1990), featuring, in an ascending stratigraphic order, the Morrona Fm, the Sabbie di Nugola Vecchia Fm and the Casa Poggio ai Lecci Fm (Mazzanti, 2016). Both the Morrona and Sabbie di Nugola Vecchia Fms are largely marine deposits of Early Pleistocene (Calabrian) age, being referred to the Santernian and Emilian regional sub-stages, respectively. Strata belonging to the Sabbie di Nugola Vecchia Fm are exposed at the Fauglia quarry (Bosio et al., 2021). The investigated succession is comprised of an alternation of sands and silts featuring, from the bottom to the top, an exceptionally preserved *Posidonia oceanica* (Linnaeus) Delile, 1813 meadow (preserving both rhyzomes and leaves), a *Cladocora caespitosa* (Linnaeus, 1767) bank and an *Ostrea edulis* Linnaeus, 1758 reef (Bosio et al., 2021). The studied barnacle specimens were originally attached to the oysters that comprise the latter reefal horizon. Palaeontological and sedimentological considerations indicate a marginal-marine, somewhat protected, progressively shallowing palaeoenvironment (Bosio et al., 2021; Mariani et al., 2022). Given the present-day bathymetric distribution of these bioconstructions (Haven and Whitcomb, 1983; Christianen et al., 2018; Kregting et al., 2020), the barnacle-rich, oyster reef-related horizon formed at 5–10 m of water depth (Bosio et al., 2021).

## 4. Material and methods

### 4.1. Geological analysis

The sedimentary successions of Pairola and Montefollonico were characterised in the field through geological and palaeontological analysis. Wherever possible, a stratigraphic section was measured with a Jacob's staff (Patacci, 2016 and references therein). Large rock samples were collected from the main lithologies, numbering 27 from Pairola and 7 from Montefollonico. Well-preserved specimens of barnacles and molluscs were collected from barnacle-dominated facies. Fossil barnacles and molluscs were also collected from the barnacle-rich layers of Certaldo, Casenuove and Fauglia. Barnacle taphonomy was investigated following the methods of Donovan (1988), Doyle et al. (1997), Nomura and Maeda (2008), Nielsen and Funder (2003) and Klompmaker et al. (2015). Carbonate rocks were classified based on Dunham's (1962) classification, which was subsequently emended by Embry and Klovan (1971) and Lokier and Al Junaibi (2016). Twenty-seven rock samples from Pairola and 25 from Montefollonico were prepared as thin sections for studying the skeletal, foraminiferal and algal assemblages. Skeletal assemblages were quantified through point-counting (Flügel, 2010), using a 250-μm-mesh and counting >500 points for each section (see Supplementary Table S1 for the raw data). Foraminiferal assemblages were studied by counting all the recognizable specimens occurring in each section (i.e., the area counting method) (Flügel, 2010; Coletti et al., 2021b) (see Supplementary Table S1 for the raw data). Wherever possible, the thickness/diameter ratio of *Amphistegina* was used as a proxy of palaeo-water depth following the approach of Mateu-Vicens et al. (2009). Coralline algal assemblages were investigated by considering the area covered by each algal taxon and using a high-rank taxonomic scheme (Aguirre et al., 2000; Coletti et al., 2018a; Coletti and Basso, 2020). Thin sections of fossil barnacle shells were also used for systematic purposes as the inner structures of the shell is characterised by taxonomically relevant microstructures (Davadie, 1963; Newman et al., 1967; Buckeridge, 1983; Coletti et al., 2019; Collareta et al., 2019, 2022).

### 4.2. Geochemical analyses on barnacle shells

In order to better appreciate the significance of the C and O stable isotope signatures of fossil barnacles, modern sessile acorn barnacles were sampled from western Liguria (*Perforatus perforatus* (Bruguière, 1789) and *Amphibalanus amphitrite* (Darwin, 1854) at Imperia; 43.88°N; 8.05°E) and along the coast of southern Tuscany (*P. perforatus* at Marina del Boccale; 43.47°N; 10.32°E; *A. amphitrite* at Livorno; 43.56°N; 10.31°E), at <1 m water depth (Fig. 1). Specimens of the epizoic barnacle *Chelonibia testudiniaria* were collected from a loggerhead turtle (*Caretta caretta* (Linnaeus, 1758)) washed ashore in Sicily (Pozzallo; 36.72°N; 14.85°E) (Fig. 1). Fossil barnacles were analysed macroscopically to evaluate their preservation state and screened for diagenetic alteration. The completeness of the shell, the homogeneity of the colour, the extent of plate preservation and the presence/absence of abrasion and/or predation boreholes were all considered for identifying the best-preserved specimens. On these bases, sessile acorn barnacles were selected from the Pairola, Montefollonico, Certaldo and Fauglia outcrops, whereas the epizoic barnacle *Chelonibia testudinaria* was selected from the Casenuove succession (Table 1).

It should be noted that, unlike other groups of fossil invertebrates (e.g., Barbin and Gaspard, 1995; Barbin, 2000; Machel, 2000; Angiolini et al., 2012; Crippa et al., 2016; Casella et al., 2018; Bosio et al., 2020; Sanfilippo et al., 2021), diagenesis in barnacles has been studied less extensively, and consequently, standard protocols for evaluating alteration in fossil barnacle remains are hitherto not available. Therefore, in order to provide clues for future researchers on how to separate pristine barnacle from altered ones, modern and fossil barnacle specimens were also analysed by means of cathodoluminescence (CL) and scanning electron microscope analysis (SEM) (Table 1). Thick sections were prepared following the procedure proposed by Crippa et al. (2016): embedding in resin, polishing with 400 and 1000 SiC, and eventually etching with diluted HCl for <15 s. A Zeiss FEG Gemini 500 SEM (Università degli Studi di Milano-Bicocca) was used for morphological observations. Secondary electron images were used to detail the structure and microstructure of modern specimens, as well as for looking for evidence of dissolution and recrystallization in the fossils. Twenty-three dedicated thin sections were prepared for optical microscope observations following the approach proposed by Collareta et al. (2019) and Coletti et al. (2019), based on cutting the same shells at different heights (Table 1). Seven such sections, which include both modern and fossil specimens from all the studied localities, were analysed through a CITL Optical CL microscope stage at the Università degli Studi di Milano-Bicocca, operated at a voltage of 6.3 kV and a current intensity of *c.* 1.1 mA, with a vacuum of *c.* 7.3 Pa.

As regards the specimens selected for isotopic analyses, sediment

**Table 1**
Sample analysed for stable isotope ratios and for the assessment of diagenetic evaluation; * indicates that the number of analysed specimens includes one of the specimens analysed for stable isotope ratios. Further information and raw data are available in Supplementary Table S1.

| Type | Locality | Barnacle stable isotopes bulk samples (n° of specimens) | Barnacle stable isotopes seasonality samples (n° of specimens) | Mollusc samples | Sediment sample | Barnacle thick section examined with SEM (n° of specimens) | Barnacle thin sections examined with optical microscope (n° of specimens) | Barnacle thin sections examined with CL (n° of specimens) |
|---|---|---|---|---|---|---|---|---|
| | Pairola | 1 | 3 | 1 pectinid<br>1 oyster<br>1 pectinid | 1 | 2* | 2* | 1* |
| | Certaldo | 2 | 3 | 1 oyster | – | 4* | 4* | 1* |
| | Casenuove | 1 | 3 | 1 oyster | – | 1* | 1* | 1* |
| | Montefollonico | 2 | 3 | 1 oyster | 1 | 2* | 4* | 1* |
| Fossil | Fauglia | 2 | 3 | 1 oyster | 1 | 2* | 4* | 1* |
| | Marina del Boccale | 1 | – | – | – | 1 | 2 | – |
| | Imperia (*A. amphitrite*) | 2 | – | – | – | 1 | 2 | – |
| | Imperia (*B. perforatus*) | 1 | 1 | – | – | 2 | 3 | 1 |
| | Livorno | 1 | 1 | – | – | 1 | 3 | 2 |
| Recent | Pozzallo | 2 | 3 | – | – | 1* | 1* | 1* |

particles cemented to the shells were gently removed using sandpaper (400 grit and subsequently 800 grit). Following Bosio et al. (2020), the specimens were then ultrasonicated in distilled water to remove any remaining particles. After drying, shell powder was collected using a hand-held microdrill equipped with a 0.8 mm metal bit with embedded synthetic diamonds. Only the cleaned external part of the shell was drilled to avoid collecting sediment and diagenetic material that might reside in the parietal tubes. In order to take into account seasonal temperature variations recorded by the fast-growing barnacle shells, several samples (4 to 7, depending on the shell size) were collected from each specimen – from the base (which represents the youngest shell part) to the top (the oldest shell part) (Fig. 2). While collecting each intra-shell sub-sample, most of the surface of the shell, excluding the sampled area, was covered in aluminum foil to avoid contamination of dust and particles originating from other parts of the shell (Fig. 2). After the collection of each sample, the shell was cleaned with pressurized air. To better assess diagenetic alteration and internal variability, several control samples were also collected and measured, namely: bulk samples collected by drilling a barnacle plate along its entire length; well-preserved associated molluscan material (either from pectinids and/or ostreids); rock samples from the barnacle-rich horizons. Stable oxygen ($\delta^{18}O$) and carbon ($\delta^{13}C$) isotope ratios were analysed with a Gas Bench II (Thermo Scientific) coupled with an IRMS Delta XP (Finnigan Matt) at the Institute of Geosciences and Earth Resources of CNR in Pisa (Italy). Carbonate samples of *c.* 0.15 mg each were dissolved in $H_3PO_4$ (105%) for one hour at 70 °C. Sample results were corrected using the international standards NBS-19 and a set of 3 internal standards (two marbles, MOM and MS, and a carbonatite, NEW12, which were previously

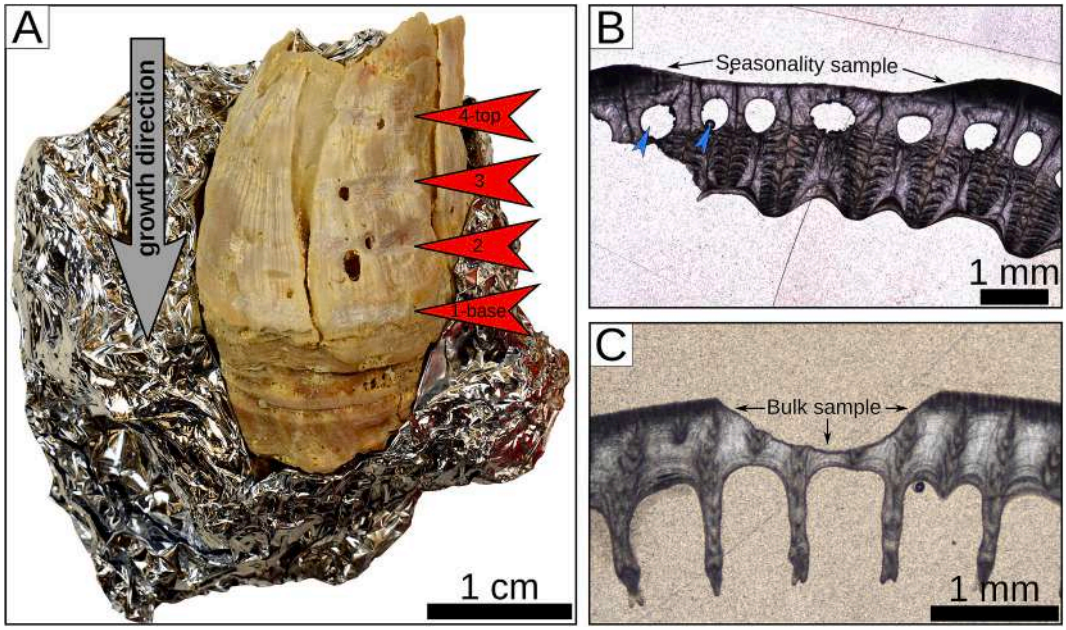


**Fig. 2.** Stable isotope sampling in barnacles. A) Intra-shell sampling for palaeoseasonality; several samples were collected from each specimen (the figured specimen was collected from the Lower Pliocene outcrop of Pairola), from the base (which represents the youngest shell part) to the top (the oldest shell part); the specimen is partially covered with aluminum foil to avoid contamination of dust and particles from other parts of the shell. B) Thin section of a fossil specimen from Certaldo, which was sampled for seasonality; the section shows how drilling is limited to the outer lamina and does not involve the parietal tubes. C) Thin section of a modern *Chelonibia* specimen from Pozzallo, from which a bulk sample (i.e., a sample crossing the entirety of the outer surface of the shell, and as such, different stages of the growth of the barnacle) was collected.

calibrated using the international standards NBS-18 and NBS-19). All the results were reported in the δ notation relative to the Vienna Pee Dee Belemnite (VPDB) international standard. Analytical uncertainties for $\delta^{18}O$ and $\delta^{13}C$ were 0.17‰ and 0.15‰, respectively (calculated as the standard deviations of the replicated analyses performed on the standards during the measurements of the investigated samples).

Raw data for C and O stable isotope ratios and point counting are included in Supplementary Table S1. Unless stated otherwise, all the analysed specimens, samples and thin sections are stored at the Dipartimento di Scienze dell'Ambiente e della Terra, Università degli Studi di Milano-Bicocca.

## 5. Results

### 5.1. Pairola succession

The Lower Pliocene succession at Pairola can be divided into two sequences (Fig. 3A). Overlaying the Upper Cretaceous turbidites that constitute the basement of the basin, the first sequence consists of boulder-rich breccias and conglomerates (dominated by clasts eroded from the underlying turbidites) (Fig. 3B-D), progressing upwards into rudstones (with a packstone matrix) (Fig. 3E-G) and, further up-section, into packstones (Fig. 3G-H). The first sequence is separated from the second by an erosional surface marked by a *Glossifungites* ichnofacies (Fig. 3I). The second sequence comprises a breccia layer that includes clasts of the underlying packstones, overlain by coarse-grained packstones and, further above, by a conglomerate layer (Fig. 3J). Two main facies, corresponding to different skeletal assemblages, can be recognised in the two sequences: a coarse-grained barnamol (BARNAcles + MOLluscs; sensu Hayton et al., 1995) (Fig. 4A, B) and a fine-grained foramol (FORAminifera + MOLluscs; sensu Lees and Buller, 1972) (Fig. 4C). The barnamol facies comprises a sizable, coarse-grained siliciclastic fraction that is mainly related to the erosion of the basement of the basin (Table 2; Fig. 4B). The bioclastic fraction is dominated by barnacles and molluscs associated with minor amounts of echinoderms, benthic foraminifera, serpulids and rare coralline algae (mainly Corallinales: *Lithophyllum*) (Table 2; Fig. 4A, B). The molluscan assemblage is dominated by moderately well-preserved oysters and pectinids associated with remnants of other recrystallized unidentified molluscs. The foraminiferal assemblage is dominated by *Cibicides* and *Elphidium*, associated with abundant *Amphistegina* and *Planorbulina*; planktic foraminifera are rare. The foramol facies also includes a relevant siliciclastic fraction, mainly consisting of sand-sized grains. The bioclastic fraction is dominated by benthic foraminifera associated with abundant echinoderms, planktic foraminifera, molluscs and barnacles (Table 2; Fig. 4C). The foraminiferal assemblage is dominated by planktic foraminifera and *Cibicides* associated with abundant *Asterigerinata* (Fig. 4D) and rarer *Amphistegina* and *Lenticulina*. Some samples display a transitional composition that is rich in both barnacles and benthic foraminifera (mainly *Cibicides* and *Amphistegina*) (Table 1; Fig. 4E, F). The barnamol facies characterizes the breccias, conglomerates and rudstones of the lower part of the first sequence as well as the uppermost conglomerate of the second sequence. The foramol facies characterizes the packstones of the uppermost part of the first sequence. The interbedded rudstones and packstones that comprise the upper part of the first sequence and the rudstones and breccias of the lower part of the second sequence host the transitional assemblage, which is rich in both barnacles and foraminifera (Fig. 3).

The barnacle assemblage of the barnamol facies is largely dominated by a single species of relatively large balanomorph balanids, up to *c.* 4 cm in height (Fig. 5). These shells, identified as *Concavus concavus* (Bronn, 1831) (Newman, 1982; Zullo, 1992; Pitombo, 2004), are globulo-conical, with ribbed triangular parietes, broad radii and a toothed, diamond-shaped orifice (Fig. 5A-C). The parietes are characterised by a single row of large parietal tubes and complex, arborescent interlaminate figures (Fig. 5D). Sutural edges display primary denticles with secondary denticles on the lower side only. The alae are cleft. Rare small individuals displaying simple interlaminate figures with a rather limited number of secondary processes have been identified as *Amphibalanus* sp. The barnacle shells are often fragmented and generally poorly preserved (Type 7 preservation of Doyle et al., 1997; Type D preservation of Nomura and Maeda, 2008) or found in small groups of relatively well-preserved specimens that are dislodged from their substrate, except when this substrate is represented by a mollusc shell (Type 2 of Doyle et al., 1997; Type C of Nomura and Maeda, 2008) (Fig. 5A-B). Opercular plates are very rare and invariably detached from the corresponding shell.

### 5.2. Certaldo succession

At Certaldo, a rather monotonous mudstone succession crops out along a partly revegetated quarry wall that erodes in a badland-like fashion (Fig. 6A). These deposits are primarily greyish-bluish, calcareous mudstones that match the original description of the "M4 muddy lithofacies" recognised by Benvenuti et al. (2014) within the sedimentary fill of the Valdelsa Basin. The succession hosts abundant macroinvertebrate fossils that concentrate in a *c.* 25 cm-thick shell bed running sub-horizontally a few meters below the top of the cliff (Fig. 6B) (Collareta et al., 2020). Invertebrate taxa from the Certaldo quarry include several bivalves and gastropods (*Bathytoma cataphracta* (Brocchi, 1814), *Calcarata calcarata* (Brocchi, 1814), *Pelecyora brocchii* (Deshayes, 1836), *Petaloconchus intortus* (Lamarck, 1818), *Tenagodus obtusus* (Schumacher, 1817) and *Thylacodes arenarius* (Linnaeus, 1758), among others) besides acorn barnacles. Vertebrates are rarer, being represented by some teeth of elasmobranchs (including *Megascyliorhinus miocaenicus* (Antunes and Jonet, 1970), *Nebriimimus wardi* Collareta et al., 2021b and *Rostroraja* sp.) as well as by bony fish otoliths (Merella et al., 2023).

Although barnacles do not represent the main component of the Certaldo macrofossil assemblage, they are relevant and occur as: (i) displaced individuals; (ii) rare individuals attached to their original substrate (i.e., other shells; Fig. 6C, D), but not in life position; (iii) disarticulated and fragmented plates (Types 2 and 7 of Doyle et al., 1997; Types C, B and D of Nomura and Maeda, 2008). Both complete individuals and fragments are generally very well preserved, showing no evidence of abrasion (Grade 0 of Nielsen and Funder, 2003), and often with remnants of the original shell colour (Fig. 6C, D). Several specimens were found with their delicate opercular plates still articulated (Fig. 6C, E). Opercular plates (both scuta and terga) are generally common in the investigated horizon (Fig. 6E, F). The assemblage is dominated by a single taxon of medium- to large-sized, conical shells with triangular parietes, broad radii and a toothed diamond-shaped orifice. Broken specimens feature a single row of large parietal tubes. The observed scuta invariably exhibit a cancellate pattern (Fig. 6E). Overall, these observations indicate that the Certaldo barnacles belong to *Concavus concavus*.

### 5.3. Casenuove succession

As the Casenuove quarry is inactive and largely covered by vegetation (Fig. 7A), our description of the outcrop is chiefly based on previous literature references (see Dominici et al., 1995; Bianucci, 1996 for a more detailed description). The base of the succession consists of coarse sands displaying high-angle cross stratification and abundant wood fragments. These are overlain by medium-grained fossiliferous sands. Further above, fine sands and bioturbated silts occur; they are characterised by a rich assemblage, including *Scrobicularia plana* (da Costa, 1778), *Striarca lactea* (Linnaeus, 1758), and shark and ray teeth. Upwards, the investigated barnacle-bearing layer is encountered. This sandy-silty layer entombs a diverse fossil assemblage, including a right whale skeleton that was excavated in 1995 (see Bianucci, 1996; Collareta et al., 2016), abundant molluscs (*Cerastodema edule*, *Bittium*

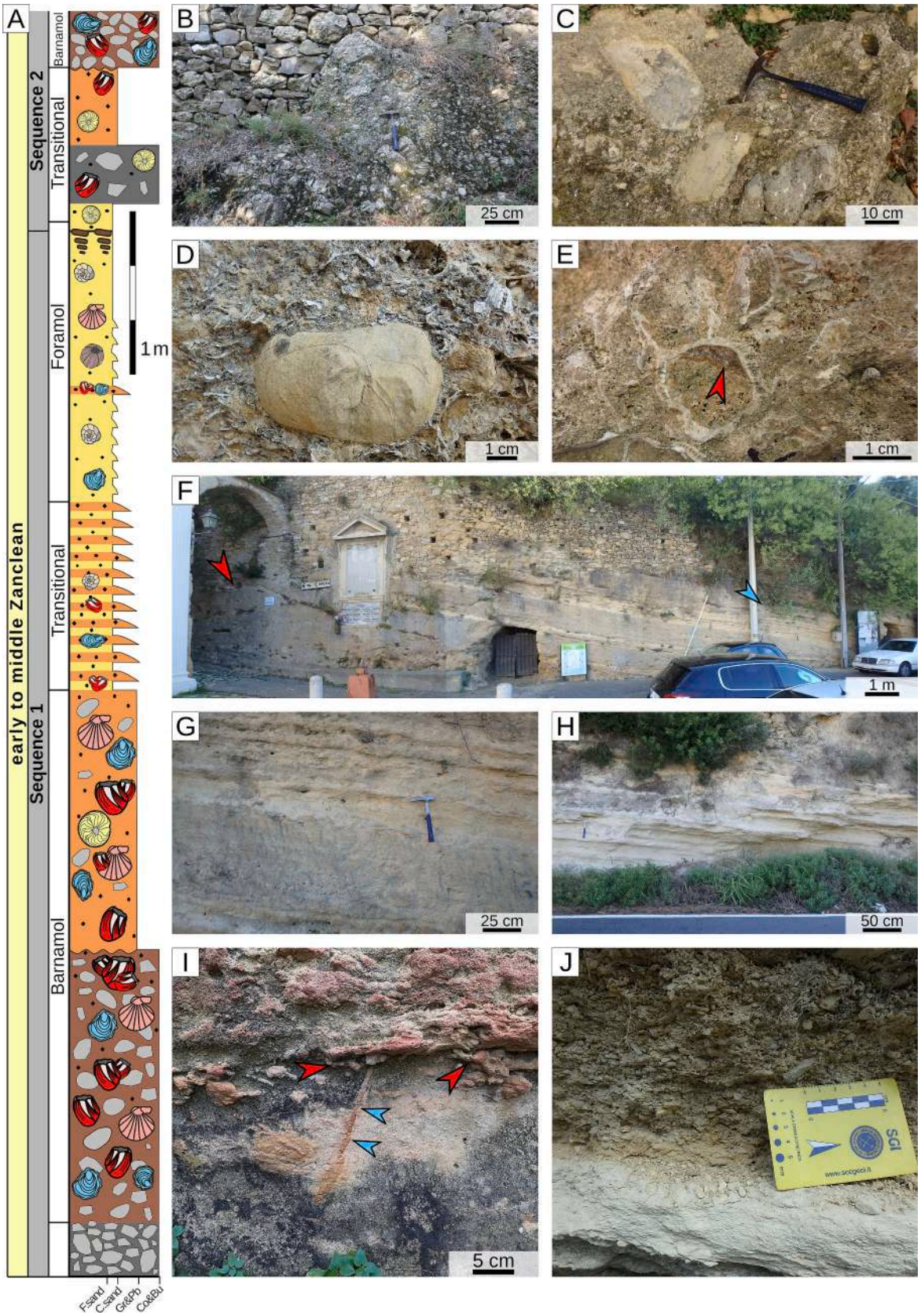


*(caption on next page)*

**Fig. 3.** Pairola succession. A) Schematic stratigraphic log of the Pairola succession, showing the main lithologies and the abundance of various bioclasts; F = fine, C = coarse, Gr = granules, Pb = pebbles, Co = cobbles, Bu = boulders; for the symbols the reader is referred to Fig. 8A. B) Basal breccia of sequence 1, which is partially covered by a dry-stone wall; the clasts of the breccia derive from the erosion of the underlying turbidites. C) Boulder-rich breccia from the base of sequence 1, characterised by an abundant bioclastic matrix displaying a barnamol assemblage. D) Detail of a bioclastic-rich conglomerate from the base of sequence 1, displaying its rich bioclastic content dominated by barnacle fragments. E) Cluster of barnacles from the lower part of sequence 1, displaying a geopetal structure (red arrowhead). F) Sequence 1; transition from the bioclastic-rich, boulder-bearing conglomerates (red arrowhead) to the overlaying rudstones with a packstone matrix that are initially interbedded with packstone layers (blue arrowhead). G) Sequence 1; detail of the rudstones with packstone matrix alternating with packstones. H) Upper part of sequence 1, dominated by packstone layers rarely interbedding with thin rudstone layers. I) *Glossifungites* ichnofacies marking the boundary between the two sequences; red arrowheads = *Thalassinoides*, blue arrowheads = *Skolithos*. J) Sequence 2; detail of the uppermost conglomerate layer. (For interpretation of the references to colour in this figure legend, the reader is referred to the web version of this article.)

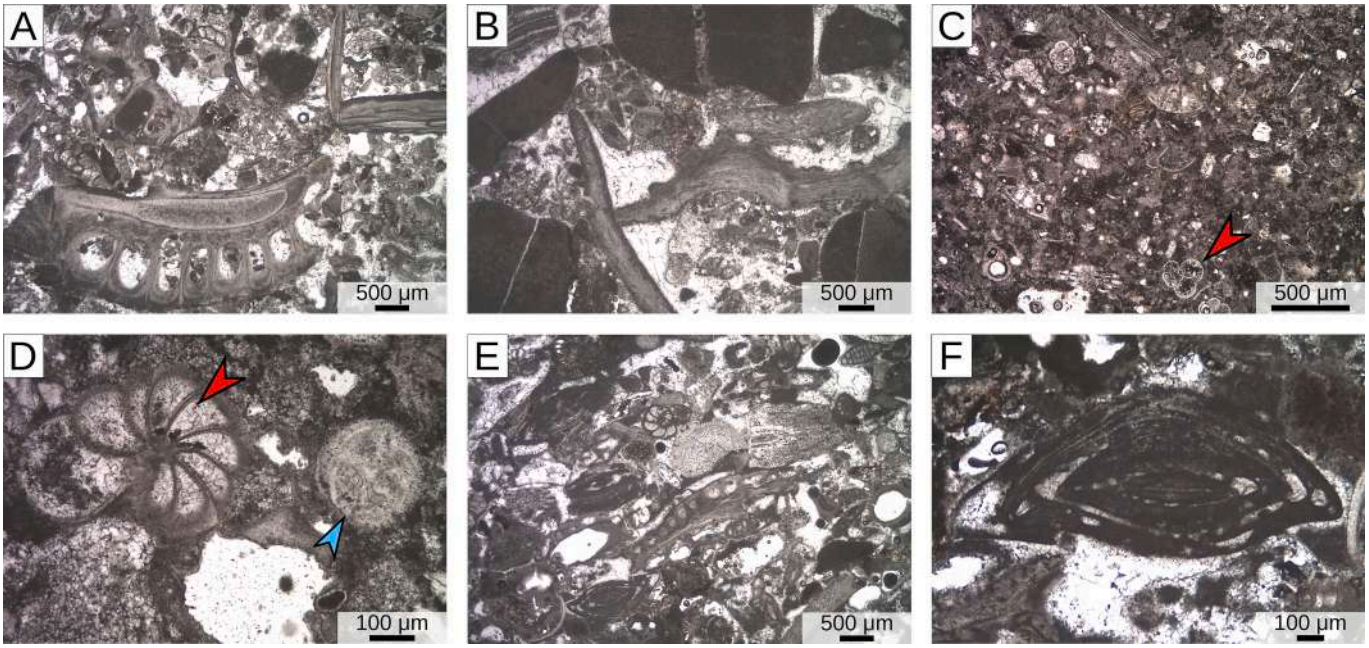


**Fig. 4.** Pairola microfacies. A) Overview of the barnamol facies, displaying a large barnacle fragment. B) Overview of the barnamol facies, displaying abundant molluscs and rock fragments. C) Overview of the foramol facies, displaying abundant planktic foraminifera (e.g., red arrowhead). D) *Cibicides* (red arrowhead) and *Asterigerinata* (basal section; blue arrowhead) from the foramol facies. E) Overview of the transitional assemblages with abundant barnacles and foraminifera. F) *Amphistegina* from the transitional assemblage. (For interpretation of the references to colour in this figure legend, the reader is referred to the web version of this article.)

*reticulatum* (da Costa, 1778), *Jujubinus exasperatus* (Pennant, 1777) and oysters), root traces and remains of decapod crustaceans. The associated microfauna is mostly represented by *Ammonia beccarii* (Linnaeus, 1758) and *Elphidium crispum* (Linnaeus, 1758). Near the whale skeleton are remains of *C. edule*, *Conus* sp., *Hadriania truncatula* (Foresti, 1868), *Paratectonatica tigrina* (Röding, 1798), *Ostrea edulis*, *Potamides tricinctus* (Brocchi, 1814), crab chelipeds and tree branches. Close to the whale skull, and especially along the right mandible, are numerous chelonibiid barnacle shells. The location of these barnacles suggests that they were attached to the skin around the jaws of the whale, and post-mortem simply dropped off when the soft tissue decomposed. Further upsection, the sequence is capped by silts and palaeosoils with sparse pulmonate gastropods.

Barnacle specimens were collected from the sediment surrounding the baleen whale skeleton, which is currently kept at the Museo di Storia Naturale dell'Università di Pisa (MSNUP) with catalogue number MSNUP I-16839 (Bianucci and Sorbini, 2014). They have been attributed to the extant *testudinaria* morph of *Chelonibia testudinaria* (Cheang et al., 2013; Zardus et al., 2014) based on the observation of the following characters: shell oval, dome-shaped, eight-plated; rostrum and rostrolatera arranged in a tripartite rostral complex; walls heavy, compartments thick and strong; radii narrow and well-sunken; sheath depending; bi-lamellar section of the parietes deep, featuring a dense pattern of longitudinal internal parietal septa whose basal edges are finely denticulated by depending points; radii distinctly notched; parietes smooth, neither ribbed nor longitudinally folded; peripheral edge neither lobed nor incised; miniature complemental males present (Collareta et al., 2016; Collareta, 2020) (Fig. 7B). From a taphonomic point of view, the epizoic nature of *C. testudinaria* and the membranous nature of its base limit the application of the taphonomic schemes of Doyle et al. (1997) and Nomura and Maeda (2008). The specimens occur both as disarticulated valves and as complete or almost complete shells. In both cases, they are usually exquisitely preserved (grade 0 of Nielsen and Funder, 2003), with pristine details of the shell morphology being retained (Fig. 7B, C).

### 5.4. Montefollonico succession

The Upper Pliocene Montefollonico succession is separated from the underlying Lower Pliocene shelf packstones by an erosional surface (Fig. 8A, B). The base of the succession consists of a normally-graded, clast-supported conglomerate displaying a large bioclastic fraction and a fine-grained micritic matrix (Fig. 8B). The conglomerate is overlain by rudstones (more coarse-grained close to the conglomerate and more fine-grained upwards) with a terrigenous fraction and a fine-grained micritic matrix (Fig. 8C-E). Both lithologies are characterised by a barnalgal facies (BARNAcles + coralline ALGae; sensu Coletti et al., 2018b) (Fig. 8D). Barnacles are more abundant in the conglomerate (Fig. 8F), whereas coralline algae and benthic foraminifera are more abundant in the rudstones (Table 2; Fig. 8G). Molluscs are also common, especially in

**Table 2**
Petrographical characteristics, skeletal assemblages and foraminiferal assemblages of the different facies that have been recognised at the Pairola and Montefollonico outcrops. Average values are indicated in bold.

| | Pairola | | | Montefollonico | |
|---|---|---|---|---|---|
| **Age** | **early to middle Zanclean** | | | **Piacenzian** | |
| **Facies** | **Barnamol** | **Transitional** | **Foramol** | **Barnalgal** | |
| Texture and lithology | Conglomerate, rudstone (packstone matrix) | Breccia, rudstone (packstone matrix), packstone | Packstone | Conglomerate | Rudstone (packstone matrix) |
| Terrigenous fraction % (average) | **40** | **40** | **15** | **65** | **15** |
| Terrigenous fraction % (min-max) | 10–80 | 15–60 | 5–35 | 60–70 | 5–45 |
| Bioclastic fraction % (average) | **60** | **60** | **85** | **35** | **85** |
| Bioclastic fraction (min-max) | 20–90 | 40–85 | 65–95 | 30–40 | 55–95 |
| **Skeletal assemblage (based on recognizable grains of the bioclastic fraction evaluated with point-counting)** | | | | | |
| Barnacles % (average) | **43** | **28.5** | **3.5** | **51.5** | **30** |
| Barnacles % (min-max) | 25–80 | 15–50 | 0–9 | 15–77 | 8–50 |
| Molluscs % (average) | **31** | **10** | **6** | **11** | **11** |
| Molluscs % (min-max) | 5–65 | 0–25 | 0–15 | 4–32 | 2–43 |
| Echinoids % (average) | **10** | **16** | **21.5** | **4.5** | **2.5** |
| Echinoids% (min-max) | 0–25 | 10–25 | 5–35 | 1–18 | 0–14 |
| Benthic foraminifera % (average) | **7** | **38** | **49** | **6** | **16** |
| Benthic foraminifera % (min-max) | 0–15 | 15–60 | 35–60 | 5–7 | 2–60 |
| Serpulids % (average) | **5** | **0** | **0** | **1.5** | **1** |
| Serpulids % (min-max) | 0–50 | // | // | 0–4 | 0–14 |
| Bryozoans % (average) | **2** | **6** | **0** | **2** | **1.5** |
| Bryozoans % (min-max) | 0–15 | 0–25 | // | 1–13 | 0–31 |
| Coralline algae % (average) | **1.5** | **0** | **0** | **23.5** | **37.5** |
| Coralline algae % (min-max) | 0–8 | // | // | 10–65 | 0–75 |
| Planktic foraminifera % (average) | **0.5** | **1.5** | **20** | **0** | **0.5** |
| Planktic foraminifera % (min-max) | 0–2 | 0–5 | 2–45 | // | 0–1 |
| **Foraminiferal assemblage (area counting)** | | | | | |
| Dominant taxa | *Cibicides-Elphidium* | *Cibicides - Amphistegina* | Planktic foraminifera-*Cibicides* | *Elphidium* – Encrusting foraminifera | *Elphidium - Ammonia - Amphistegina* |
| Amphistegina T/D ratio (average) | // | **0.40** | **0.36** | // | **0.40** |
| Amphistegina T/D ratio (min-max) | // | 0.32–0.44 | 0.33–0.41 | // | 0.29–0.54 |
| Planktic/Benthic ratio (average) | **0.06** | **0.08** | **1.21** | **0.01** | **0.002** |
| Planktic/Benthic ratio (min-max) | 0–0.15 | 0–0.16 | 0.2–2.63 | 0–0.02 | 0.001–0.003 |

the rudstones where molds of large specimens can be observed (Fig. 8E); except for rare oysters, most of the observed molluscs are obviously recrystallized. Echinoderms and serpulids are rare. The foraminiferal assemblage is dominated by elphidiids; *Cibicides* and *Asterigerinata* are also common (Table 2). *Ammonia* and *Amphistegina* are common in the rudstones (Fig. 8H, I), whereas encrusting foraminifera are common in the basal conglomerate. Both lithologies contain small miliolids, which often exhibit different types of partial dissolution. Coralline algae occur as coated grains growing over pebbles and shells (including barnacles shells) as well as small rhodoliths with branched morphology. In the conglomerate, the algal assemblage is dominated by Corallinales (88%; mainly *Lithophyllum*), with small amounts of Hapalidiales (12%; mainly *Roseolithon*) (Fig. 8J). The algal assemblage of the rudstones is dominated by Hapalidiales (62%; mainly *Roseolithon*, *Mesophyllum* and *Lithothamnion*) associated with abundant Corallinales (38%; mainly *Lithophyllum*) (Fig. 8K, L).

Barnacles are usually moderately well preserved (Fig. 9A), especially in the rudstones where specimens still retaining traces of their original colour were collected. Barnacles occur as (i) displaced clusters; (ii) clusters attached to their original substrate (including pebbles, and rhodoliths) although not in life-position; and (iii) disarticulated plates and fragmented plates (Types 2 and 5 of Doyle et al., 1997; Types C and D of Nomura and Maeda, 2008; grades 0 to 1 of Nielsen and Funder, 2003). The assemblage is dominated by medium- to large-sized, conical shells with triangular parietes, broad radii and a toothed, diamond-shaped orifice (Fig. 9A, B). Specimens observed in thin section feature a single row of large parietal tubes and complex, arborescent interlaminate figures (Fig. 9C). Abundant opercular plates (mainly scuta, but a pair of terga were also recovered) are dispersed in the sediment; most of the scuta display a cancellate pattern (Fig. 9B). Overall, these observations indicate that the Montefollonico barnacle palaeocommunity was dominated by *Concavus concavus*.

### 5.5. Fauglia succession

The Lower Pleistocene succession of Fauglia consists of sands and silts that were deposited in a nearshore coastal environment characterised by a seagrass meadow (lower part of the succession; Fig. 10A), a *Cladocora caespitosa* bank (upper part; Fig. 10B) and an *Ostrea edulis* reef overlain by shoreface sands (capping the succession; Fig. 10C) (Bosio et al., 2021; Mariani et al., 2022). Barnacles encrust the oysters of the reef and mainly occur as articulated shells (Fig. 10D), sometimes still

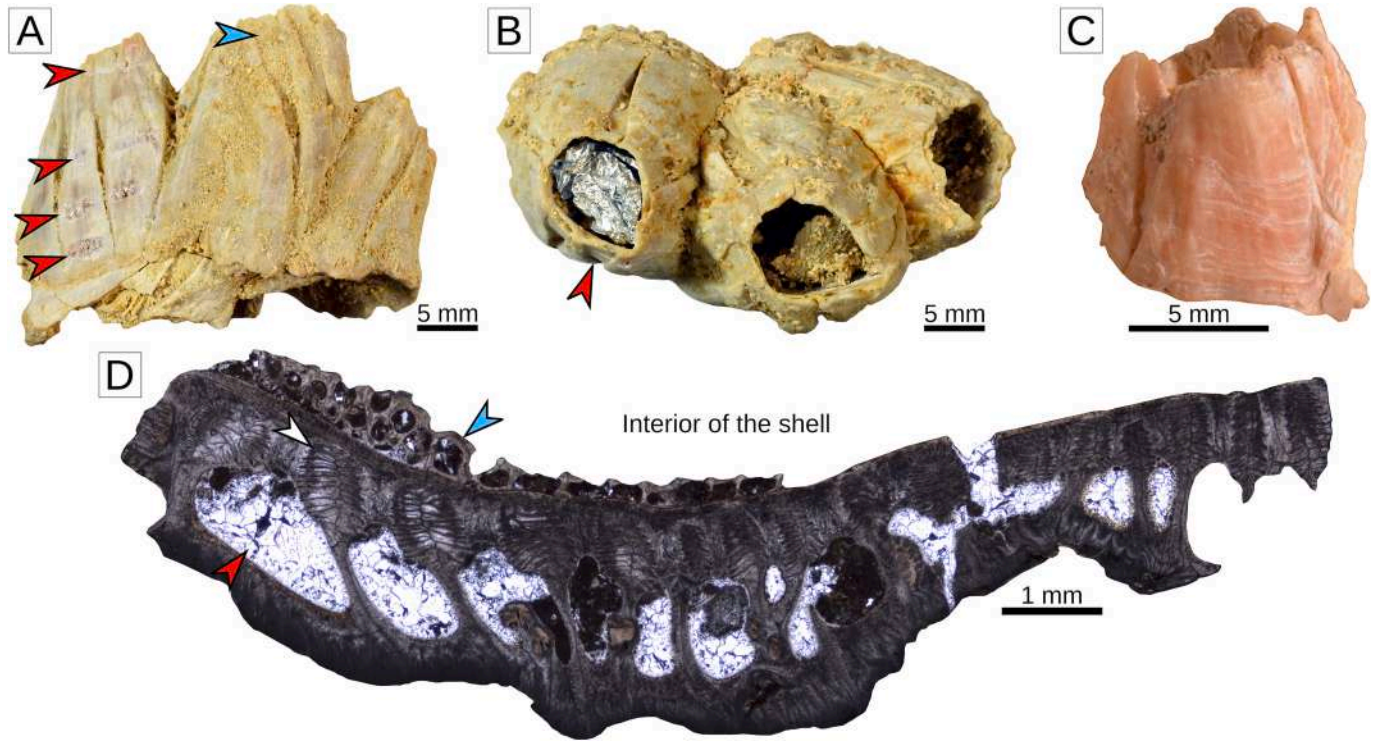


**Fig. 5.** Barnacle assemblage from the barnamol facies of the Pairola outcrop. A) Cluster including three well-preserved specimens of *Concavus concavus*; one of the surfaces of the leftmost specimen has been cleaned and sampled for stable isotope analysis to study palaeoseasonality (red arrowheads); note the broad radii (blue arrowhead). B) Apical view of the same cluster as in panel A; red arrowhead indicates the specimen sampled for stable isotope analysis, displaying a well-preserved, diamond-shaped orifice. C) Small, solitary specimen of *C. concavus* preserving remnants of the original shell colour. D) Thin section of a parietal plate of *C. concavus*, displaying the single row of large parietal tubes and complex, arborescent, interlaminate figures (white arrowhead); red arrowhead = parietal tube filled by sparitic calcite crystals; blue arrowhead = bryozoan colony encrusting the inner surface of this disarticulated barnacle plate. (For interpretation of the references to colour in this figure legend, the reader is referred to the web version of this article.)

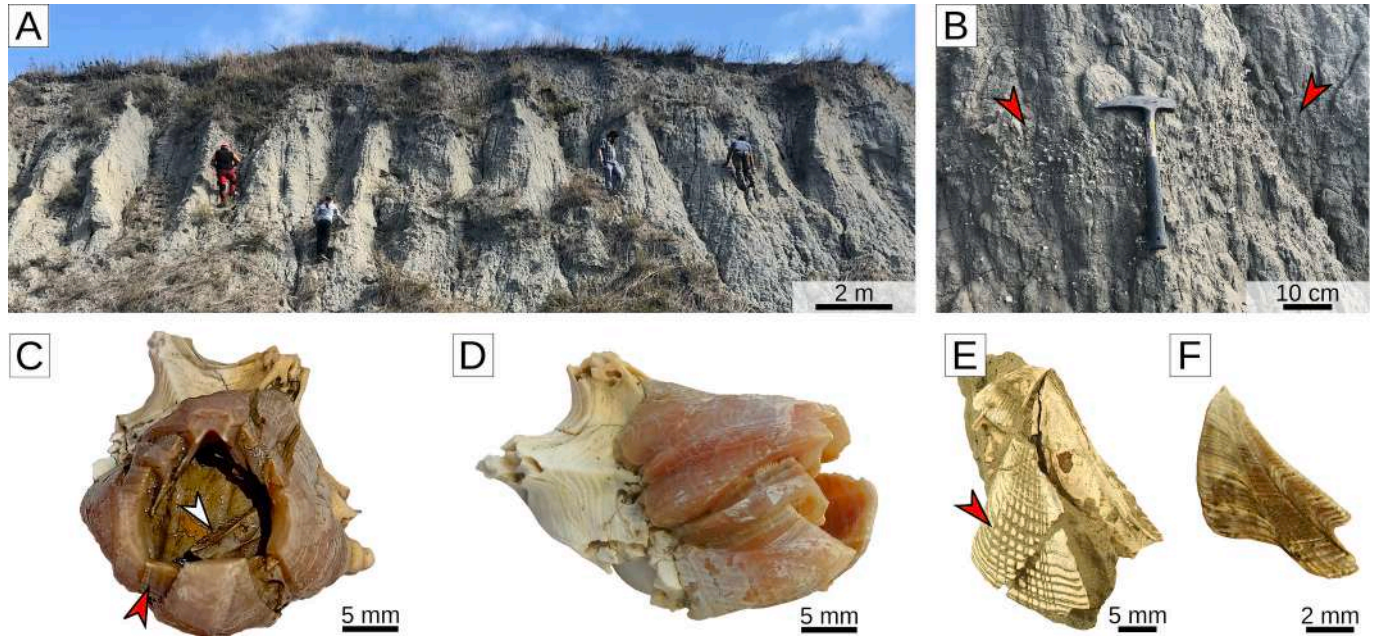


**Fig. 6.** Certaldo outcrop and barnacles. A) Overview of the outcrop, with calcareous mudstones eroding in a badland-like fashion. B) Shell-rich bed (red arrowheads). C) Apical view of a well-preserved specimen of *Concavus concavus* attached to a gastropod shell and still displaying its pinkish colour; note the broad radii (red arrowhead) and the presence of an opercular plate (white arrowhead) still within the diamond-shaped orifice of the shell. D) Lateral view of the same specimen as in panel C. E) Articulated pair of delicate opercular plates, including a scutum exhibiting a cancellate pattern (red arrowhead). F) A tergum from one of the examined *C. concavus* specimens. (For interpretation of the references to colour in this figure legend, the reader is referred to the web version of this article.)

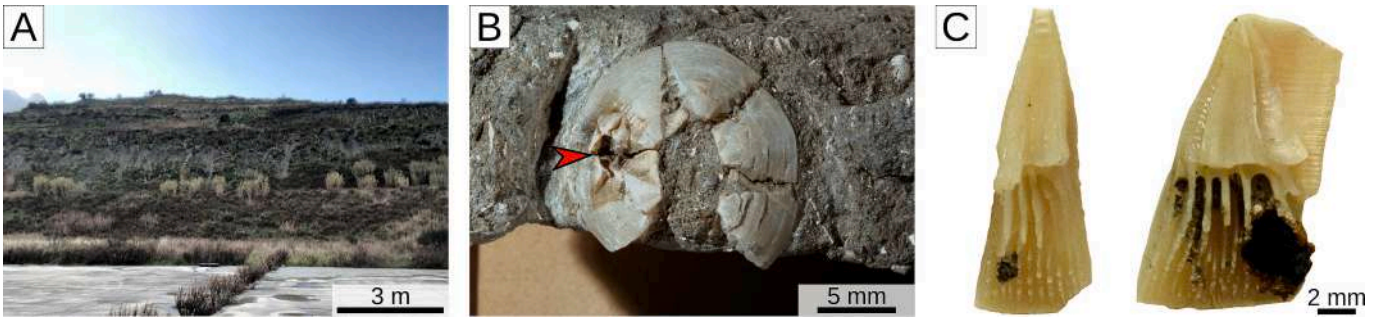


**Fig. 7.** Casenuove outcrop and barnacles. A) Overview of the outcrop. B) Well-preserved specimen of *Chelonibia testudinaria*, displaying delicate features such as a complemental male (red arrowhead) and the embedding fine-grained sediment. C) *Chelonibia testudinaria* rostral plates, displaying their glossy and well-preserved inner surface. (For interpretation of the references to colour in this figure legend, the reader is referred to the web version of this article.)

possessing their opercular plates (Type 1 of Doyle et al., 1997; Type A of Nomura and Maeda, 2008). The shells display no evidence of abrasion (Grade 0 of Nielsen and Funder, 2003), but some appear to have been compressed and deformed during diagenesis. The observed specimens are small to medium-sized, and characterised by conical shells with triangular parietes, narrow radii and a proportionally small orifice (Fig. 10E). The scuta display pronounced transverse growth lines and lack radial striae (Fig. 10F). On the basis of these characters, the Pleistocene Fauglia barnacles are assigned to the extant Mediterranean species *Perforatus perforatus*.

### 5.6. C and O stable isotope ratios

Modern Western Mediterranean barnacle specimens (*Perforatus perforatus*, *Amphibalanus amphitrite* and *Chelonibia testudiniaria*) exhibit similar isotopic ranges, with $\delta^{13}C$ values ranging between −0.8‰ and + 1.5‰ and $\delta^{18}O$ values ranging between −1.1‰ and + 2.4‰ (Fig. 11). Fossil barnacle specimens exhibit a much larger range, namely, between −7.6‰ and + 2.4‰ in $\delta^{13}C$ and between −4.8‰ and + 2.3‰ in $\delta^{18}O$ (Fig. 11). No sub-set of samples, in its entirety, display a very strong correlation between the $\delta^{13}C$ and $\delta^{18}O$ values. The fossil barnacles from Pairola range between −5.5‰ and − 4.0‰ in $\delta^{13}C$, and between −4.6‰ and − 2.7‰ in $\delta^{18}O$, exhibiting a correlation between the two variables ($R^2 = 0.85$, $n = 13$). These values match the coeval oyster sample ($\delta^{13}C = -4.2$‰; $\delta^{18}O = -4.2$‰) as well as the embedding sediment ($\delta^{13}C = -4.6$‰; $\delta^{18}O = -4.3$‰), while the bulk barnacle specimen ($\delta^{13}C = -1.6$‰; $\delta^{18}O = -0.4$‰) and the coeval pectinid bivalve ($\delta^{13}C = -0.4$‰; $\delta^{18}O = -1.5$‰) display different values. The fossil barnacles from Fauglia, which were sampled for seasonality, range from −7.6‰ to −2.6‰ in $\delta^{13}C$, and from −3.7‰ to +0.3‰ in $\delta^{18}O$. They also display a correlation between $\delta^{13}C$ and $\delta^{18}O$ ($R^2 = 0.91$, $n = 12$). The co-occurring oyster sample has much higher values ($\delta^{13}C = +0.2$‰; $\delta^{18}O = +0.1$‰), while the sediment and the barnacle bulk sample are near the lower end of the range of the seasonality samples. In the cases of Fauglia and Pairola, the vast majority of the barnacle data fall outside the known range of living calcareous cirripedes. Fossil barnacles from Montefollonico range between −3.9‰ and + 1.2‰ in $\delta^{13}C$, and between −4.0‰ and − 0.3‰ in $\delta^{18}O$. They display a weak correlation between $\delta^{13}C$ and $\delta^{18}O$ ($R^2 = 0.3$, $n = 17$). The co-occurring oyster, sediment and bulk barnacle samples display values consistent with those of barnacles sampled for seasonality. In this case, the isotopic values of the fossil barnacles fall almost entirely within the range of living calcareous cirripedes but outside the range of the analysed modern barnacles from the Western Mediterranean (Figs. 11, 12). The fossil barnacles from Certaldo range between +1.0‰ and + 1.9‰ in $\delta^{13}C$, and between +1.6‰ and + 2.3‰ in $\delta^{18}O$, exhibiting a very low value of $R^2$ ($R^2 = 0.16$, n = 17). The co-occurring oyster sample has different values ($\delta^{13}C = +2.4$‰; $\delta^{18}O = +1.0$‰), whereas the bulk barnacle sample falls within the range displayed by the seasonality samples. Overall, the fossil barnacles from Certaldo are within the range of living cirripedes and almost within that of the investigated living barnacles from the Western Mediterranean (Fig. 12A). The fossil specimens of *Chelonibia testudinaria* from Casenuove range between −1.6‰ and + 1.9‰ in $\delta^{13}C$, and between 1.1‰ and + 1.3‰ in $\delta^{18}O$, exhibiting a very low value of $R^2$ ($R^2 = 0.16$, $n = 15$). The co-occurring oyster sample has similar values ($\delta^{13}C = -0.6$‰; $\delta^{18}O = -1.2$‰), and the bulk barnacle sample falls within range of the seasonality samples. The Casenuove specimens also display values that are entirely comparable to those of their living counterparts (Fig. 12B). However, while all the analysed specimens of living *C. testudinaria* are characterised by $\delta^{18}O$ values that become progressively higher throughout life, specimens “a” and “c” from Casenuove display $\delta^{18}O$ values that seemingly decrease progressively (Fig. 12B), with specimen “b” displaying a mixed pattern (Fig. 12B).

### 5.7. Analysis of the barnacle shell microstructure

Conventional optical microscopy does not highlight any relevant structural differences among the investigated shell barnacles, nor does it reveal any extensive evidence of recrystallization (Fig. 13A-I). The shell wall always consists of an inner and an outer lamina, and is permeated by parietal tubes (Fig. 13A-I); the internal upper part of the shell displays a sheath of variable thickness adjacent to the inner lamina (Fig. 13E). Complex growth lines and interlaminate figures can be seen in different parts of the shells (Fig. 13A-I). SEM observations at low magnification show the same general structure and highlight no major differences between modern and fossil specimens (Fig. 13J). At higher magnification it is possible to observe that the microstructure of the shell of modern specimens (both epizoic and non-epizoic) consists of scale-like elements (1 to 5 μm long and *c.* 1 μm thick) that are arranged in complex patterns (hereinafter referred to as the “dragon-scale” pattern) (Fig. 13K-T). This organization results in the growth lines that are observed under the optical microscope at lower magnification. The scales are relatively loosely packed, with irregular spaces and crevices between one another (Fig. 13M, O, Q, T). Furthermore, nano-scale porosity can be observed within the scales themselves (Fig. 13M, O). A similar pattern can be observed in specimens from Montefollonico (Fig. 13U-X). However, here the scales are bulkier and have poorly defined margins when compared to modern specimens (Fig. 13W). This is more pronounced in the Certaldo specimens (Fig. 13Y, Z), and even more so in the epizoic specimens from Casenuove (Fig. 13 AA). In the Pairola specimens, the dragon-scale pattern is completely obliterated, and no clear organization of the microstructure can be observed (Fig. 13 BB, CC). The specimens from Fauglia display different levels of preservation of the microstructure, ranging from completely obliterated (Fig. 13 DD, EE), like in the Pairola specimens (Fig. 13 CC), to relatively well preserved (Fig. 13 FF, GG), like in the Montefollonico specimens (Fig. 13W, X). CL observations show that modern barnacles (both epizoic and non-epizoic froms) are usually non-luminescent, except for

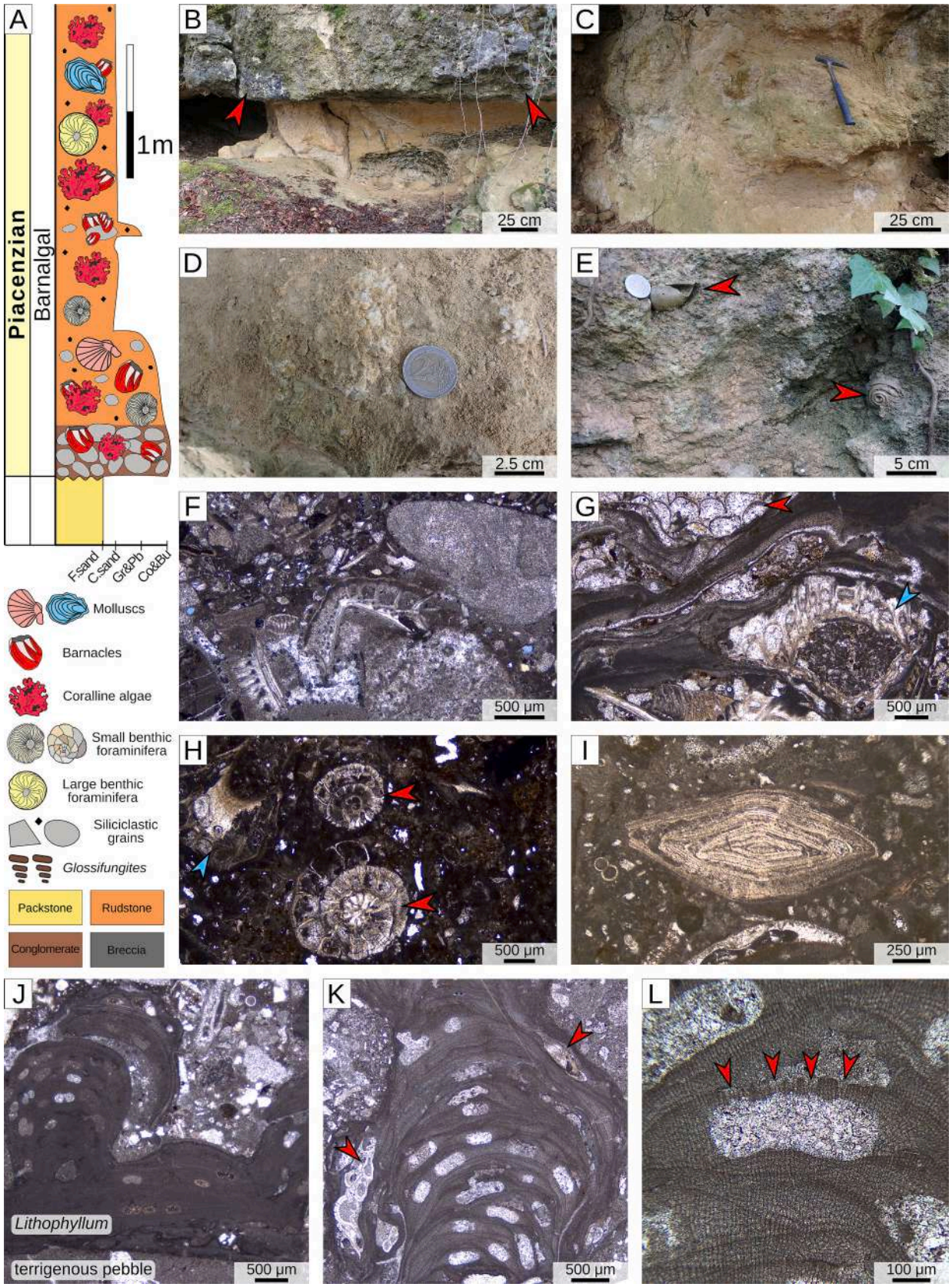


*(caption on next page)*

**Fig. 8.** Montefollonico outcrop and microfacies. A) Schematic stratigraphic log of the outcrop, indicating the main lithologies and the abundance of various bioclasts. B) The basal conglomerate of the succession (red arrowhead), which is separated from the underlying Lower Pliocene packstone by an erosional surface. C) Overview of the barnalgal rudstones. D) Detail of a barnacle-encrusted rhodolith from the rudstones. E) Large gastropod molds (red arrowhead) observed within the rudstones. F) Microfacies of the barnalgal conglomerate, displaying abundant barnacle and rock fragments. G) Microfacies of the barnalgal rudstone, displaying a barnacle (blue arrowhead), encrusted by coralline algae, which in turn are encrusted by bryozoans (red arrowhead). H) Microfacies of the barnalgal rudstone, displaying large specimens of *Ammonia* cut along almost equatorial sections (red arrowheads) and a barnacle plate (blue arrowhead). I) Microfacies of the barnalgal rudstone, displaying large specimens of *Amphistegina*. J) Specimen of *Lithophyllum* growing over a pebble in the basal conglomerate. K) Specimen of *Roseolithon* from the rudstones; the red arrowhead indicates an encrusting hyaline foraminifera. L) Detail of the multiporate conceptacles of *Roseolithon*, displaying the characteristic roof pits created by degenerate rosette cells surrounding the pore canals (Coutinho et al., 2022). (For interpretation of the references to colour in this figure legend, the reader is referred to the web version of this article.)

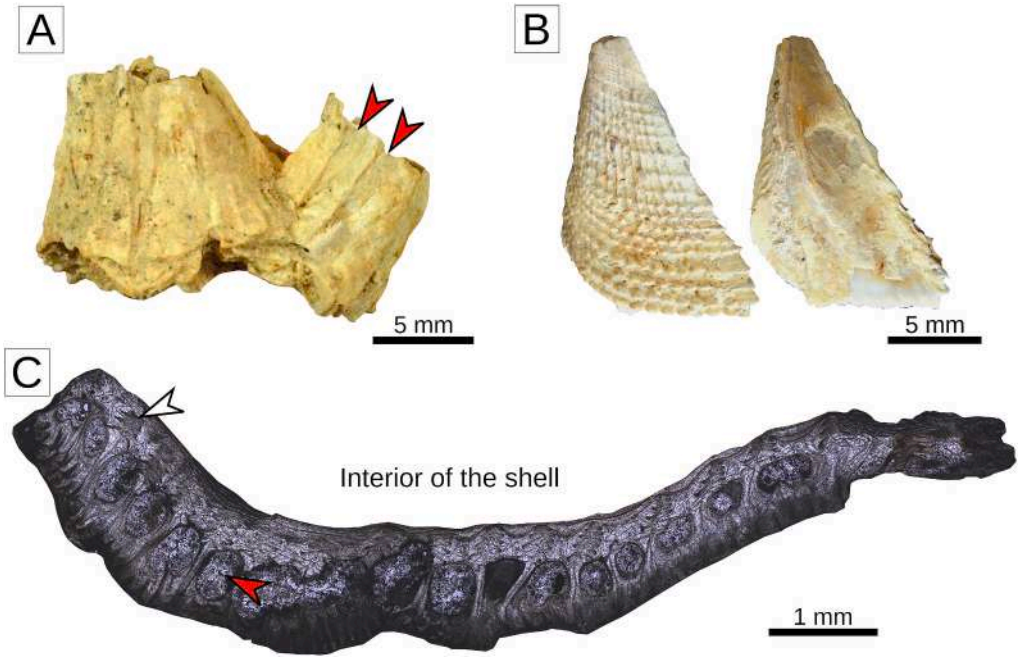


**Fig. 9.** Montefollonico barnacles. A) Small cluster of moderately preserved specimens of *Concavus concavus*; red arrowheads indicate the broad radii. B) Views of the external and internal (reflected) surfaces of a scutum, displaying a cancellate pattern on the external surface. C) Thin section of a parietal plate of *C. concavus*, displaying the single row of large parietal tubes and its complex, arborescent, interlaminate figures (white arrowhead); red arrowhead indicates a parietal tube filled by sparitic calcite crystals. (For interpretation of the references to colour in this figure legend, the reader is referred to the web version of this article.)

the inner lining of the parietal tubes and the outer lining of the inner lamina, where very weak luminescence can be observed (Fig. 14A-F). Similar to the modern specimens, the fossil barnacles from Montefollonico, Certaldo and Casenuove do not display a strong luminescence (Fig. 14G-L). The specimens from Certaldo and Casenuove only display a very faint glow in correspondence of growth lines around the inner surface of the parietal tubes, the outer surface of the inner lamina, and along the interlaminate figures (Fig. 14I-L). The specimens from Montefollonico exhibit a weak luminescence along the inner lamina and the interlaminate figures, and display luminescent parietal tubes partially filled by diagenetic calcite (Fig. 14G-H). The examined specimen from Pairola displays parietal tubes filled by sparitic calcite, and is clearly luminescent similar, to the associated oysters (Fig. 14M-P). In turn, the examined specimen from Fauglia displays a strong luminescence and parietal tubes filled by sparitic calcite (Fig. 14Q, R).

## 6. Discussion

### 6.1. Palaeoenvironmental reconstruction

The skeletal assemblage of the Montefollonico succession is dominated by barnacles (especially the basal conglomerate) and coralline algae (Tables 1, 2; Fig. 8). Barnacle-dominated facies commonly occur in <15–20 m water depth, while facies rich in both barnacles and coralline algae are known to occur also in slightly deeper settings (MacIntyre and Milliman, 1970; Milliman, 1972; Coletti et al., 2018b). The coralline algal assemblage of the basal conglomerate is dominated by Corallinales, whereas in the rudstones both Hapalidiales and Corallinales are abundant. In oligotrophic tropical settings, similar assemblages would correspond to a water depth of 0–20 m (for the conglomerate) and 40–60 m (for the rudstones); however, Hapalidiales-dominated assemblages can occur in shallower settings at higher latitudes and/or in turbid water (Adey and Macintyre, 1973; Minnery et al., 1985; Adey, 1986; Aguirre et al., 2000; Coletti and Basso, 2020). Based on the presence of the large benthic foraminifera *Amphistegina* (Beavington-Penney and Racey, 2004; Triantaphyllou et al., 2009; Langer et al., 2012), the Montefollonico succession should have deposited in a warm-temperate to subtropical setting. The abundant detrital material suggests terrestrial runoff and an elevated nutrient supply. Non-oligotrophic conditions are also suggested by barnacle abundance itself (Sanford and Menge, 2001; Michel et al., 2011; Reijmer et al., 2012; Reynaud and James, 2012; Reymond et al., 2016; Coletti et al., 2018b). Since in temperate and/or nutrient-rich settings Hapalidiales dominance is observed at shallower depths than in oligotrophic tropical settings (Aguirre et al., 2000; Coletti et al., 2018a; Coletti and Basso, 2020), a water depth of about 20 m can be envisioned for the barnalgal conglomerate, and of 20–40 m for the barnalgal rudstones (Table 3). This is consistent with the taxonomic composition of the Hapalidiales assemblage, which features genera such as *Mesophyllum* and *Roseolithon* that usually occur at intermediate depth (Adey, 1986; Iryu, 1992;

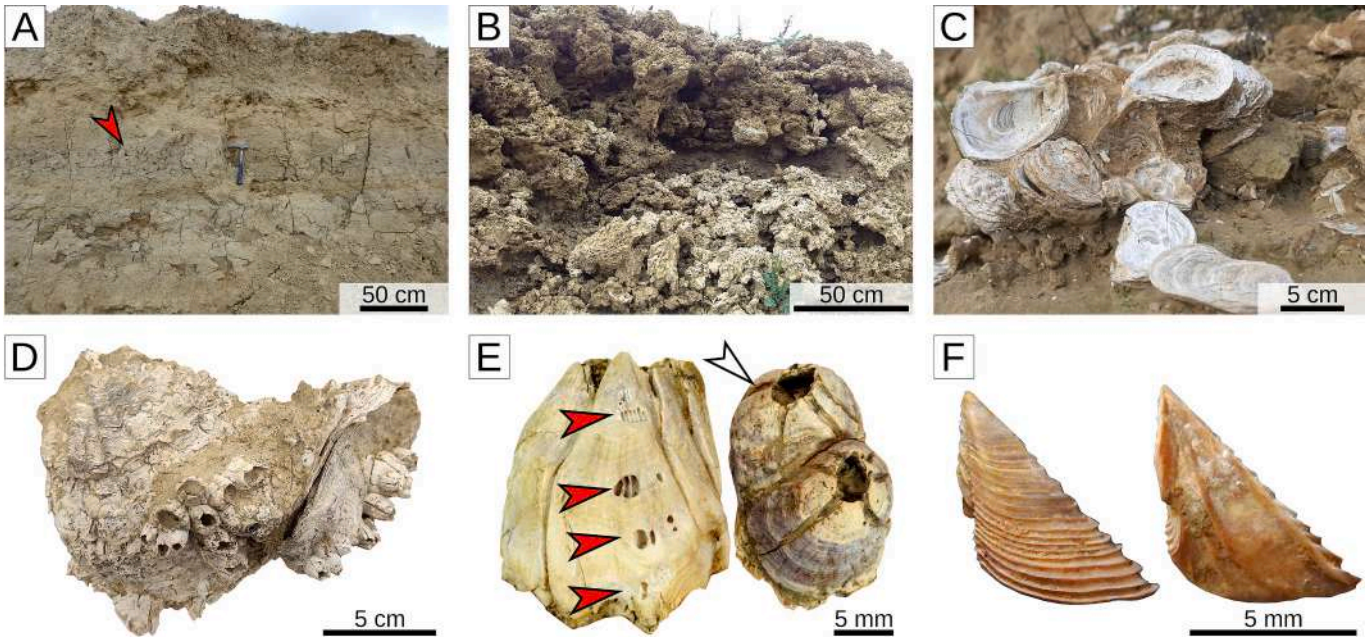


**Fig. 10.** Fauglia outcrop and barnacles. A) Seagrass meadow from the lower part of the succession; the red arrowhead indicates seagrass rhizomes. B) *Cladocora caespitosa* bioconstruction from the upper part of the succession. C) Cluster of oysters from the oyster reef at the top of the succession. D) Barnacle-encrusted oysters from the oyster reef. E) Specimens of *Perforatus perforatus*; the one on the left of the panel was sampled for stable isotope analyses; red arrowheads indicate the sampling points; white arrowheads indicate the narrow radius. F) Views of the external and internal (reflected) surfaces of a scutum of *P. perforatus*. (For interpretation of the references to colour in this figure legend, the reader is referred to the web version of this article.)

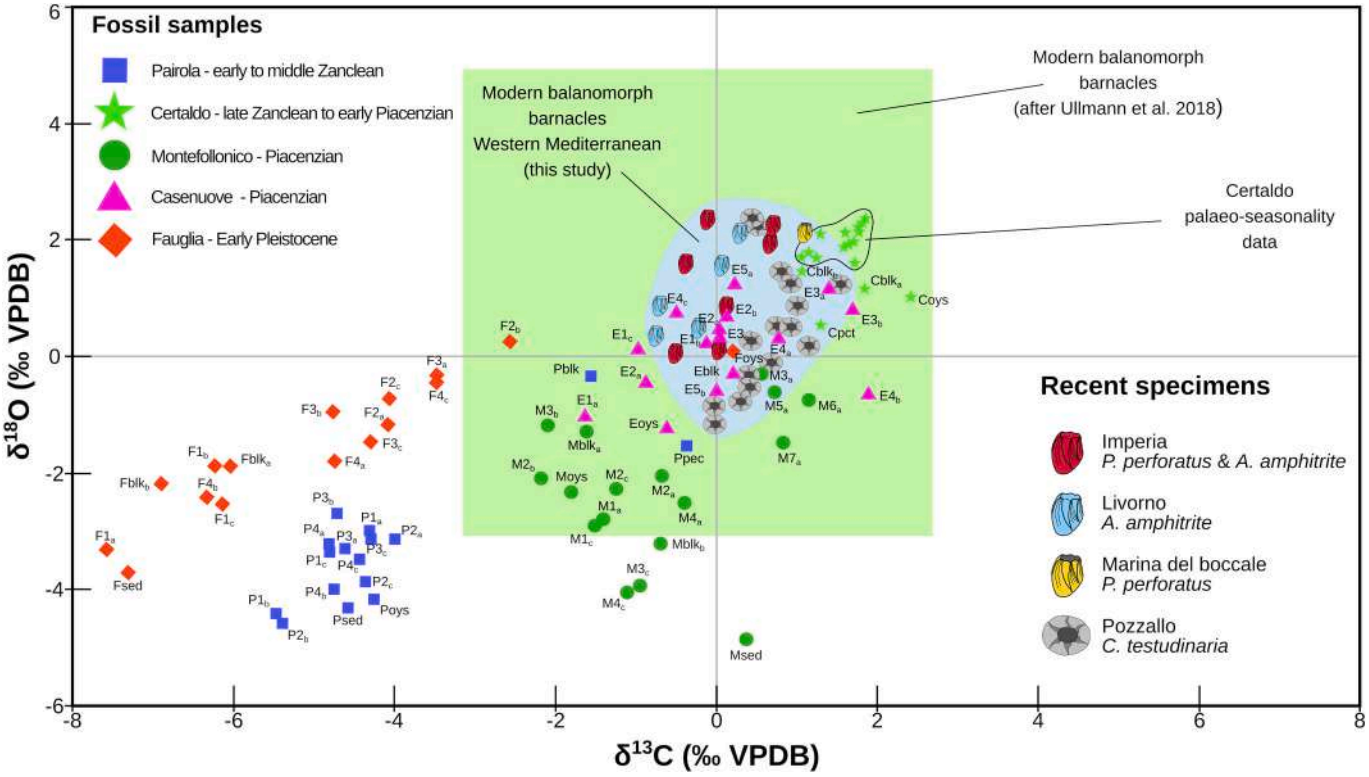


**Fig. 11.** $\delta^{18}O$ and $\delta^{13}C$ values for the investigated fossil samples and various modern balanomorph barnacles; in the label of the samples P = Pairola, C = Certaldo, M = Montefollonico, E = Casenuove, F = Fauglia, oys = oyster, pct = pectinid, blk = bulk, sed = embedding sediment; the number following the first letter in the label of seasonality samples indicates the position of the intra-shell sample with respect to the base of the shell, with 1 representing the intra-shell sample closer to the base of the shell (and thus the youngest part thereof); the following letter indicates the specimen.

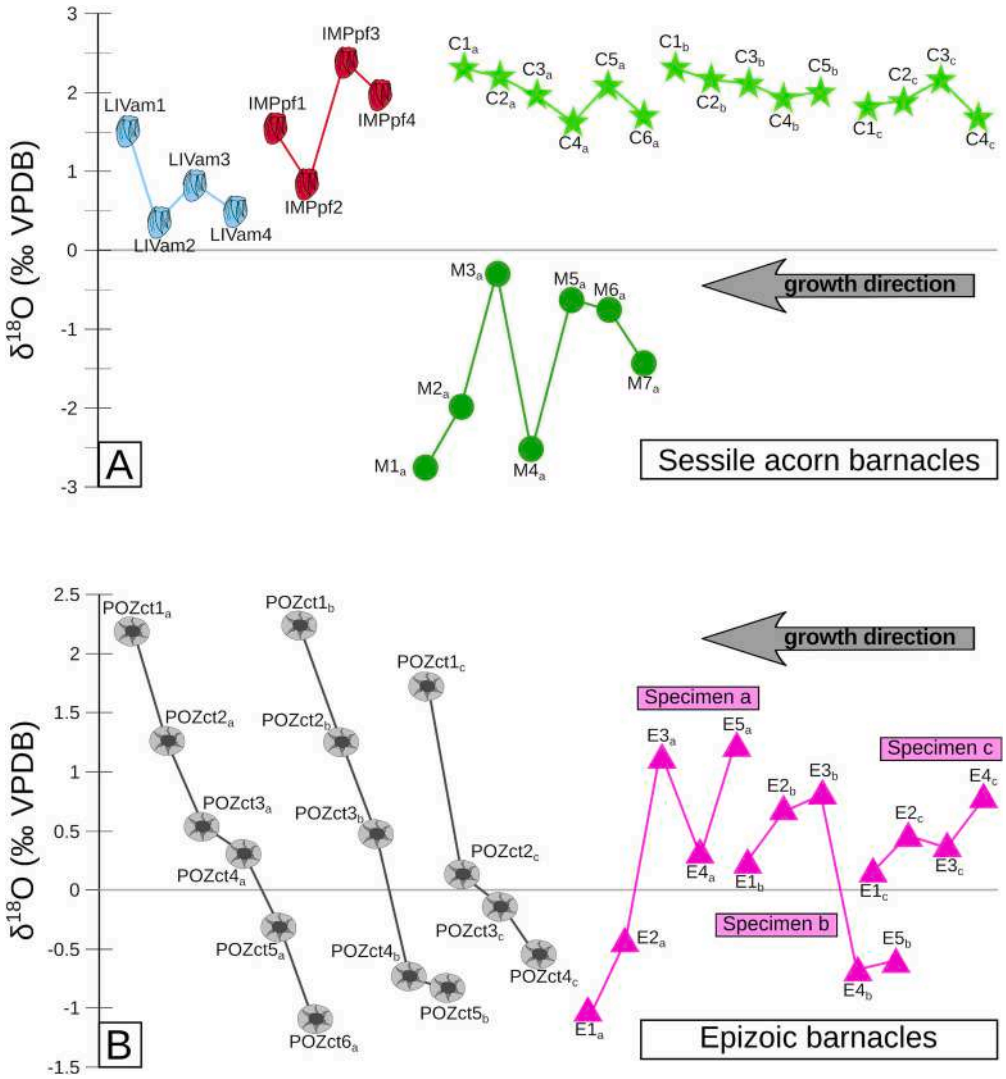


**Fig. 12.** Stable isotope composition of some selected specimens. A) $\delta^{18}O$ record of the analysed modern specimens of *Amphibalanus amphitrite* from Livorno, modern specimens of *Perforatus perforatus* from Imperia, Piacenzian fossils of *Concavus concavus* from Montefollonico, and mid-Pliocene fossils of *C. concavus* from Certaldo. B) $\delta^{18}O$ record of the analysed modern specimens of *Chelonibia testudinaria* from Pozzallo and the middle Piacenzian fossils of *C. testudinaria* from Casenuove. Key to the figure is the same as in Fig. 11.

Cabioch et al., 1999; Basso et al., 2009; Coletti et al., 2016, 2018a). This reconstruction is also consistent with the foraminiferal assemblage, which is dominated by shallow-water taxa and lacks both deep-water and planktic taxa. The thickness/diameter ratio of *Amphistegina* can also provide information on water depth as it decreases with decreasing light availability due to either increasing water depth or increasing turbidity (Mateu-Vicens et al., 2009) (Table 2). Following Mateu-Vicens et al.'s (2009) equations, this parameter suggests a water depth comprised between 5 and 20 m (assuming eutrophic conditions), or between 10 and 35 m (assuming mesotrophic conditions), further supporting the palaeobathymetric consideration based on barnacles and algae. Barnacle taphonomy and preservation, together with the general abundance of micrite, suggests a relatively sheltered setting characterised by limited post-mortem reworking of the bioclasts.

Based on the previously stated criteria for palaeoenvironmental reconstruction, the barnamol facies of Pairola most likely formed in <15 m water depth, that is, a slightly shallower setting than that of the barnalgal rudstones of Montefollonico (Tables 1, 2; Figs. 3, 4). Shallower conditions are suggested by: (i) higher abundance of barnacles and lower abundance of coralline algae; (ii) a coralline algal assemblage that entirely consists of Corallinales. Furthermore, the lack of micrite and poorer barnacle preservation suggest that the Pairola barnamol probably formed in a high-energy setting. Indeed, the barnacles from Pairola are almost invariably detached from their former substrate and opercular plates are rare, whereas the barnacles from Montefollonico are often found still attached to their substrate (e.g., rhodoliths, molluscs and pebbles) and opercular plates are relatively common. Such a difference in hydrodynamic energy is consistent with the more sheltered and protected nature of the Neogene basins of central Tuscany (e.g., Nalin et al., 2010, 2016) compared to those of Western Liguria, the latter being more exposed to waves and currents (Coletti et al., 2021a). Similar to the Montefollonico succession, the Pairola succession displays a decrease in the abundance of both barnacles and terrigenous grains moving away from the coast. As barnacle-dominated carbonate factories usually flourish in nearshore settings along rocky coasts (Coletti et al., 2018b), within barnacle-dominated carbonate systems the overall abundance of barnacle remains can be used as a proxy for water depth and distance from the coastline. The main exceptions to this model are represented by accumulations resulting from the extensive downslope transportation of shallow-water elements (Buckeridge et al., 2018a) and deep-water barnacle communities (Buckeridge, 1999). The former are relatively common in carbonate systems lacking a marginal rim, but can

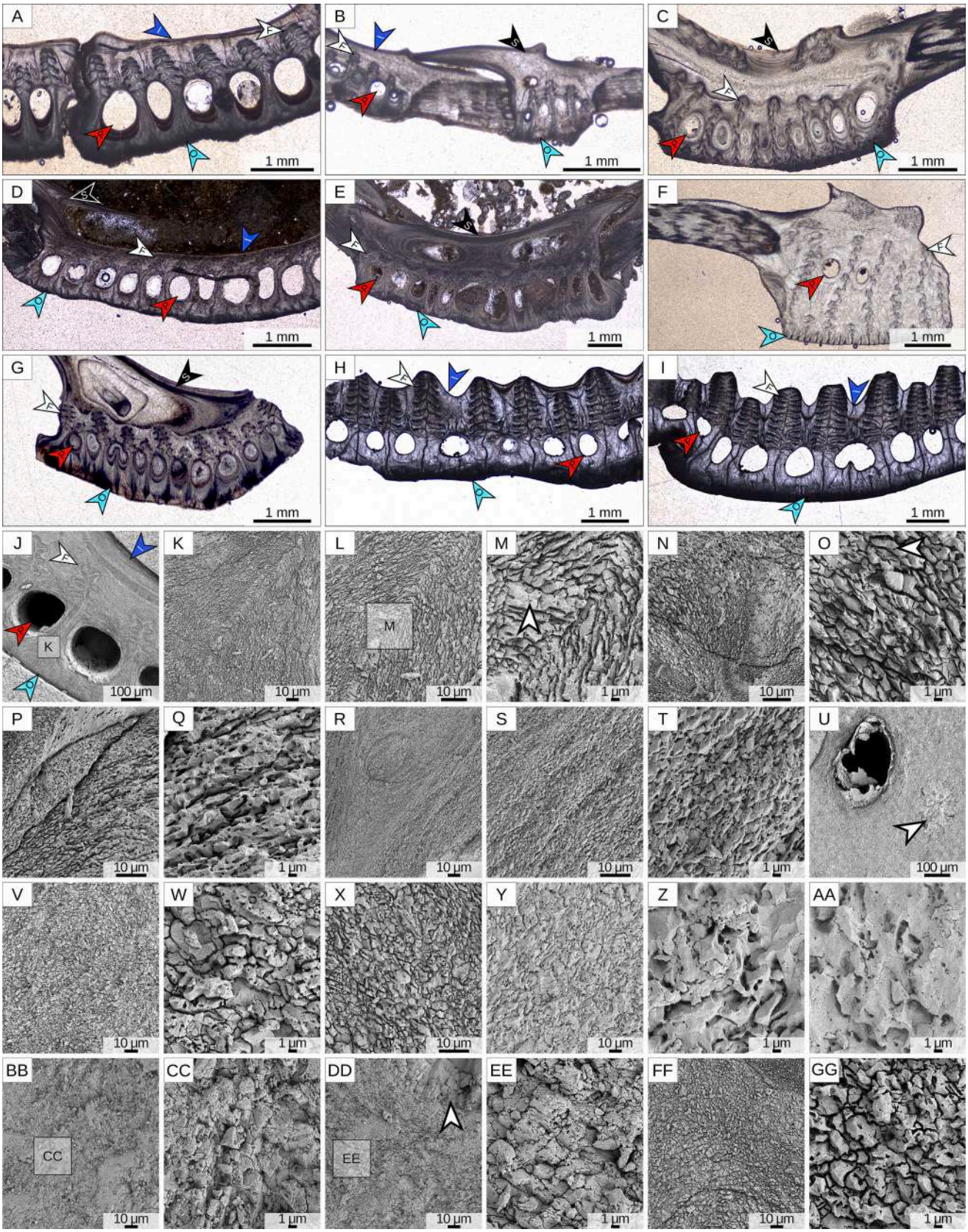


*(caption on next page)*

**Fig. 13.** Analysis of barnacle microstructure with optical microscope and SEM; dark blue arrowhead I = inner lamina; light blue arrowhead O = outer lamina; red arrowhead P = parietal tube; white arrowhead F = interlaminate figure; black arrowhead S = sheath. A) *Perforatus perforatus*, modern specimen from Imperia. B) *Amphibalanus amphitrite*, modern specimen from Livorno. C) *Chelonibia testudinaria*, modern specimen from Pozzallo. D) *P. perforatus*, fossil specimen from Fauglia, analysed for stable isotope ratios. E) *Concavus concavus*, fossil specimen from Pairola, analysed for stable isotope ratios. F) *C. testudinaria*, fossil specimen from Casenuove, analysed for stable isotope ratios. G) *C. concavus*, fossil specimen from Montefollonico, analysed for stable isotope ratios. H) *C. concavus*, fossil specimen from Certaldo, analysed for stable isotope ratios. I) *C. concavus*, same specimen as in panel H; this slice is located slightly closer to the apex of the shell, thus representing a slightly older shell part compared to the one in panel H. J) *A. amphitrite*, modern specimen from Imperia; inset panel indicates the position of panel K. K) *A. amphitrite*, same specimen as in panels J, L, M; note the growth lines arising from the arrangement of the scales. L) *A. amphitrite*, same specimens as in panels J, K, M; note the growth lines arising from the arrangement of the scales; inset panel indicates the position of panel M. M) *A. amphitrite*, same specimen as in panels J, K, L; note the dragon-scale arrangement of the scales of low magnesium calcite constituting the shell; white arrowhead = intra-scale porosity. N) *P. perforatus*, same specimen from Imperia as in panel A. O) *P. perforatus*, detail of panel N highlighting the dragon-scale pattern; white arrowhead = intra-scale porosity. P) *P. perforatus*, detail of a sheath of a modern specimen from Marina del Boccale. Q) *P. perforatus*, detail of panel P highlighting the dragon-scale pattern. R) *C. testudinaria*, same specimen from Pozzallo as in panel C; note the growth lines arising from the arrangement of the scales. S) *C. testudinaria*, detail of panel R. T) *C. testudinaria*, detail of panel S highlighting the dragon-scale pattern. U) *C. concavus*, same fossil specimen from Montefollonico as in panel G; white arrowhead = parietal tube filled by sparitic cement. V) *C. concavus*, detail of panel U. W) *C. concavus*, detail of panel V, highlighting the dragon-scale sheatpattern characterised by scale slightly bulkier and more porous than those of modern specimens. X) *C. concavus*, detail of the sheath, same fossil specimen as in panels G, U, V, W. Y) *C. concavus*, same fossil specimen as in panels H, I. Z) *C. concavus*, detail of panel Y, highlighting the altered dragon-scale pattern with scales bulkier and less defined than those of the Montefollonico specimen in panel W. AA) *C. testudinaria*, same fossil specimen as in panel F; note the altered dragon-scale pattern with scales bulkier and less defined than those of the Certaldo fossil specimen of *C. concavus* in panel Z. BB) *C. concavus*, same fossil specimen from Pairola as in panel E; notice the chaotic arrangement and the lack of clearly recognizable patterns; inset panel indicates the position of panel CC. CC) *C. concavus*, detail of panel BB highlighting the chaotic structure and the complete alteration of the original microstructure. DD) *P. perforatus*, same fossil specimen as in panel D; note the chaotic arrangement and the lack of clearly recognizable patterns; inset panel indicates the position of panel EE. EE) *P. perforatus*, detail of panel DD highlighting the chaotic structure and the complete alteration of the original microstructure. FF) *P. perforatus*, another fossil specimen from Fauglia (different from the previous one); inset panel indicates the position of panel GG. GG) *P. perforatus*, detail of panel FF, highlighting the relatively well preserved dragon-scale pattern. (For interpretation of the references to colour in this figure legend, the reader is referred to the web version of this article.)

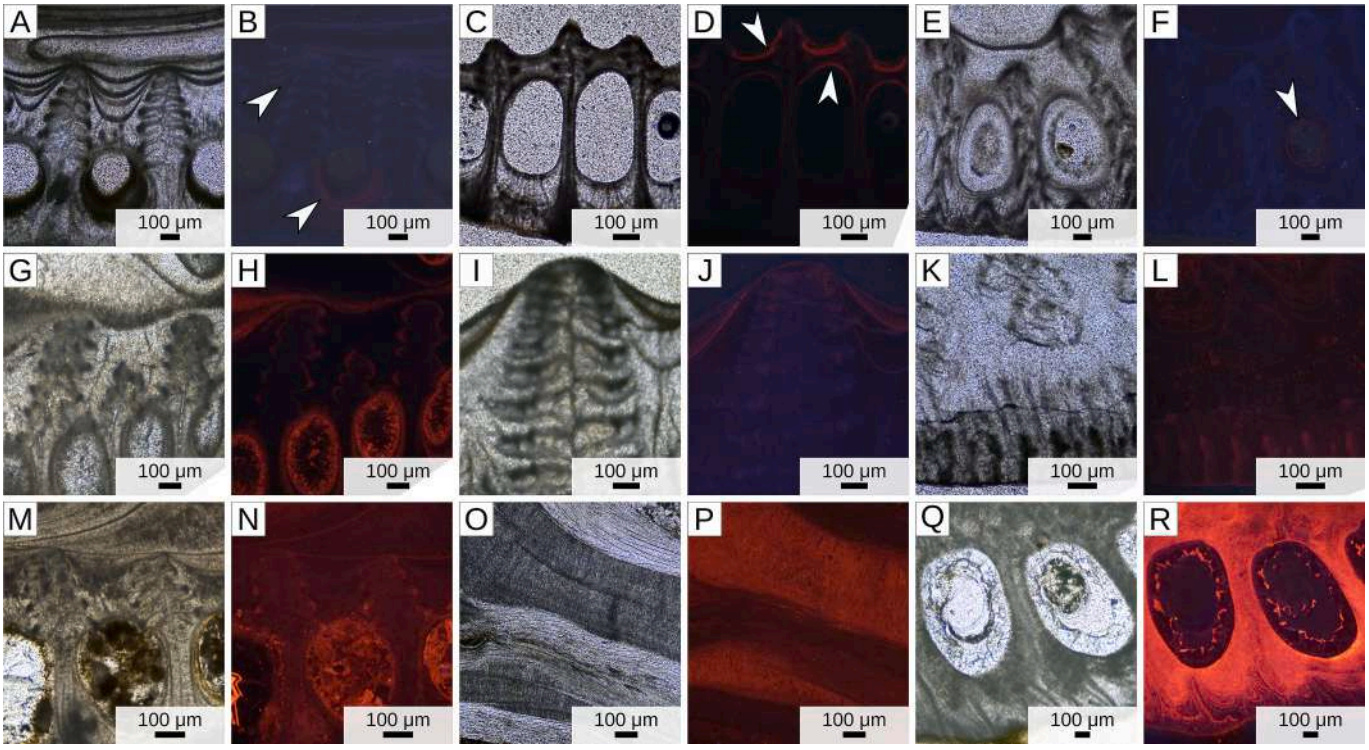


**Fig. 14.** CL analysis of barnacle structures. A) *Perforatus perforatus*, modern specimen from Imperia, also depicted in Fig. 13A. B) *P. perforatus*, same specimen as in panel A, observed in CL; white arrowheads indicate the very faint glow in correspondence of growth lines around the inner surface of the parietal tubes and the interlaminate figs. C) *Amphibalanus amphitrite*, modern specimen from Livorno, also depicted in Fig. 13B. D) *A. amphitrite*, same specimen as in panel C, observed in CL; white arrowheads indicate the very faint glow in correspondence of growth lines around the inner surface of the parietal tubes, the outer surface of the inner lamina and along the interlaminate figs. E) *Chelonibia testudinaria*, modern specimen from Pozzallo, also depicted in Fig. 13C. F) *C. testudinaria*, same modern specimen as in panel E, observed in CL; white arrowheads indicate the very faint glow in correspondence of growth lines around the inner surface of the parietal tubes. G) *Concavus concavus*, fossil specimen from Montefollonico, also depicted in Fig. 13G. H) *C. concavus*, same fossil specimen as in panel G, observed in CL. I) *C. concavus*, fossil specimen from Certaldo, also depicted in Fig. 13H, I. J) *C. concavus*, same fossil specimen as in panel I, observed in CL. K) *C. testudinaria*, fossil specimen from Casenuove, also depicted in Fig. 13F. L) *C. testudinaria*, same fossil specimen as in panel K, observed in CL. M) *C. concavus*, fossil specimen from Pairola, also depicted in Fig. 13E. N) *C. concavus*, same fossil specimen as in panel M, observed in CL. O) Ostreid from the Pairola barnamol facies. P) Ostreid, same fossil specimen as in panel O, observed in CL. Q) *P. perforatus*, fossil specimen from Fauglia, also depicted in Fig. 13D. R) *P. perforatus*, same fossil specimen as in panel Q, observed in CL.

**Table 3**
Palaeoenvironmental and stratigraphic summary of the different investigated outcrops.

| Site | Age | Type of barnacle accumulation | Setting | Water depth | Lithology | Barnacle taphonomy |
|---|---|---|---|---|---|---|
| Pairola | early - middle Zanclean | Barnacle-dominated facies | High-energy, nearshore coastal setting | 0–15 m | Coarse-grained, mixed siliciclastic bioclastic | Poorly preserved (rarely well preserved); detached from their substrate; opercular plates very rare and always disarcticulated |
| Certaldo | late Zanclean - early Piacenzian | Barnacle-rich layer | Low-energy, open shelf setting | > 40 m | Shell-rich calcareous mudstone | Well preserved; sometimes attached to their substrate; opercular plates common and sometimes articulated |
| Casenuove | middle Piacenzian | Barnacle-rich layer | Low-energy, nearshore coastal embayment | 0–10 m | Shell-rich calcareous sandy siltstone | Very well preserved; close to their original substrate; pristine details of the shell preserved |
| Montefollonico | Piacenzian | Barnacle-dominated facies | Moderate-energy, nearshore coastal setting | c.a. 20 m | Coarse-grained, dominantly siliciclastic | Moderately preserved; generally detached from their substrate; opercular plates present but always disarticulated |
| Montefollonico | Piacenzian | Barnacle-dominated facies | Moderate-energy, coastal setting | 20–40 m | Coarse-grained, mixed siliciclastic bioclastic | Moderately preserved; often attached to their substrate; opercular plates common but always disarticulated |
| Fauglia | Early Pleistocene | Barnacle-rich oyster reef | Moderate-energy, nearshore coastal setting (possibly a coastal embayment) | 5–10 m | Coarse-grained, mixed siliciclastic bioclastic | Moderately to well preserved; often attached to their substrate; opercular plates common and sometimes articulated |

be recognised due to the mixture of both deep and shallow water taxa and on the basis of barnacle taphonomy (Buckeridge, 2015; Buckeridge et al., 2018a). The latter are less frequent and can be identified thanks the peculiar internal structure of deep-water barnacles, which lack parietal tubes (Buckeridge, 1999). In addition to these main exceptions, accumulations of shells of epizoic barnacles, whose distribution is mostly explained by the environmental preferences, movement patterns, removal behaviour and post-mortem taphonomy of the host organisms, also exist worldwide (e.g., Bianucci et al., 2006; Buckeridge et al., 2018b). As proposed by Collareta et al. (2016), the many shells of *C. testudinaria* from Casenuove may be representative of such an accumulation.

Both the barnacle-rich *Ostrea edulis* reef of Fauglia and the barnacle-bearing deposit of Casenuove should have formed in very-shallow settings, most likely <10 m in light of their molluscan assemblages (Símonarson, 1981; Haven and Whitcomb, 1983; Christianen et al., 2018; Kregting et al., 2020) (Table 3; Figs. 7, 10). On the other hand, the Certaldo mudstones most likely formed into deeper conditions (Table 3; Fig. 6). As proposed by previous authors (Benvenuti et al., 2014; Dominici et al., 2018), these structureless deposits formed most likely in an offshore setting, at depths of a few tens of meters. Strengthening this interpretation, the *Concavus concavus* shells from this locality are exquisitely preserved, which is consistent with no transportation and wave-related reworking. Some of the shell even feature articulated opercula (Fig. 6), further supporting the absence of relevant currents at the seafloor.

From the palaeoclimatic point of view, the barnacle facies from Pairola and Montefollonico and the barnacle rich-layers from Certaldo and Casenuove formed in a warm-temperate to subtropical climate as suggested by the presence of *Amphistegina* (Pairola and Montefollonico) and the coeval vertebrate assemblages (Certaldo and Casenuove) (Dominici et al., 1995; Rustioni and Mazza, 2001; Collareta et al., 2020, 2021a, 2021b). This is consistent with the published literature on the studied area (Nalin et al., 2010, 2016) and the overall warm climate of the Mediterranean area during the Pliocene (Prista et al., 2015). The Lower Pleistocene succession of Fauglia was deposited under colder conditions compared to the other successions. This is suggested by the lack of symbiont-bearing foraminifera, such as *Amphistegina*, *Sorites* and *Peneroplis* (Mariani et al., 2022), and is consistent with the Early Pleistocene climatic deterioration (e.g., Lisiecki and Raymo, 2007). The shallow-water barnacle assemblages of the Western Mediterranean were affected by this climatic event. Pliocene barnacle assemblages were largely dominated by *C. concavus* (Aguirre et al., 2008; Radwańska and Radwański, 2008; Coletti et al., 2021a; this work); however, during the Early Pleistocene, *C. concavus* became rarer and eventually went extinct (Menesini, 1965; Newman, 1982; Zullo, 1992) to be possibly replaced by other Concavinae such as the extant *Perforatus perforatus*. Such a pattern suggests a preference for warm conditions for *C. concavus* as well as its potential as a proxy of warm-temperate to subtropical palaeoclimates.

### 6.2. C and O stable isotope ratios

Both the oxygen- and carbon-isotope ratios of the modern Western Mediterranean barnacles exhibit a narrower variation range compared to those reported by Ullmann et al. (2018) for barnacles worldwide (Fig. 11). Isotopic values from Casenuove and Certaldo fall mostly within the range of the modern Western Mediterranean samples, whereas the samples from Montefollonico are almost within the broader range of modern barnacles from various localities worldwide (Figs. 11, 12). The samples from Fauglia and Pairola fall outside the range of all modern barnacles by displaying very low values of $\delta^{13}C$ and $\delta^{18}O$, which in turn is strongly suggestive of the interaction with fresh water (Sharp, 2017) (Fig. 11). Overall, the barnacle samples from Fauglia, Montefollonico and Pairola were probably altered by meteoric waters or diagenetic fluids. This is supported by the strong correlation that is observed between $\delta^{13}C$ and $\delta^{18}O$ (e.g., Knauth and Kennedy, 2009) in the barnacle samples from Fauglia and Pairola (Fig. 11), as well as by the results of the SEM and CL investigations, which clearly indicate significant alteration (Figs. 13, 14).

The $\delta^{18}O$ values of the Certaldo specimens of *Concavus concavus* slightly differ from those of *Perforatus perforatus*, i.e., their closest Mediterranean living relative. On average, the Certaldo barnacles display higher isotopic values and much smaller intra-specimen variations (Fig. 12A). The oxygen isotope composition of marine biogenic carbonates depends on the temperature of carbonate precipitation (e.g., Epstein et al., 1953), with which it is inversely correlated, as well as on the oxygen-isotope composition of seawater, which in turn depends on the global ice volume (with lower $\delta^{18}O$ values corresponding to smaller ice caps; e.g., Shackleton, 1987) and salinity changes (reflecting evaporation, freshwater dilution and mixing of water masses; e.g., Railsback et al., 1989). Both temperature and salinity vary on a seasonal basis, thus $\delta^{18}O$ changes on annual profiles of sessile organisms can be seen as a proxy for seasonality (e.g., Ivany, 2012). During the Pliocene, in the Mediterranean region as well as globally, the climate was warmer than now (Plancq et al., 2015; Prista et al., 2015). The reduced seasonality expected during time intervals with limited ice caps might thus explain the observed limited intra-specimen variations, but the warm climate of the Pliocene should correspond to lower rather than to higher $\delta^{18}O$ values. It should be noted that the barnacles we are comparing belong to two different genera, and as such, they may record different vital effects

with respect to the oxygen and carbon isotope fractionation. Assuming neither large salinity variations (see below) nor large differences in vital effects, another possible explanation that can justify both the reduced intra-specimen variability (a proxy of seasonality) and the increase in the average value of $\delta^{18}O$ (a proxy of temperature) relies in slightly different life habits for the two groups of barnacles. The examined specimens of *P. perforatus* were collected at about 1 m water depth, hence well above the thermocline. Sedimentological and palaeontological observations suggest that the Certaldo individuals of *C. concavus* lived below the wave base at a depth of a few tens of meters, and as such, in relatively colder water where thermal seasonality was likely buffered.

Pliocene and modern specimens of *Chelonibia testudinaria* feature similar values and ranges of intra-specimen variability, but display a different pattern (Fig. 12B). Moving from the youngest to the oldest part of the shell, the Pliocene specimens are characterised by an irregular increase of $\delta^{18}O$, whereas the modern ones show the opposite trend. This likely reflects differences in the seasonal movement patterns of the barnacles' hosts: the modern specimens from Pozzallo were collected from a loggerhead turtle, whereas those from Casenuove were most likely attached to the right whale near which they have been found (Collareta et al., 2016).

As already mentioned, salinity is also known to affect the $\delta^{18}O$ value of biogenic shells (Railsback et al., 1989). Concerning the epizoic barnacles, this has been exploited, in combination with the effect of temperature, to track the movements of the barnacle's host across different parts of its biogeographic range, as long as these areas are several hundreds of kilometres apart from one another (Killingley, 1980; Killingley and Lutcavage, 1983; Newman and Killingley, 1985; Detjen et al., 2015; Pearson et al., 2019, 2020). However, even in the most recent analyses, the effects of temperature and salinity could not be separated from each other (Pearson et al., 2019). The observed fossil assemblages of Montefollonico, Pairola and Certaldo do not display remarkable evidence for relevant and prolonged salinity variations. On the other hand, prolonged non-euhaline conditions cannot be excluded for the barnacle-rich oyster reef of Fauglia. Here, meteoric diagenesis altered the C and O stable isotope composition of the shells. Therefore, among the studied specimens, only those from Casenuove could display intra-shell variations that are potentially related to salinity. However, lacking a well constrained relationship between $\delta^{18}O$ salinity and temperature in modern barnacles as well as an accurate model of salinity variations in the Mediterranean during the Pliocene, detailed interpretations would be entirely speculative.

Analyses of the barnacle microstructure indicate that conventional microscope observation does not allow to separate pristine samples from those that have been altered (Fig. 13). In turn, the SEM and CL analyses permitted the recognition of the most severely altered specimens (i.e., Fauglia and Pairola), and provided some clues for detecting specimens with an intermediate degree of alteration (i.e., Montefollonico). The sedimentological context also proved to be highly informative for the preservation state of the specimens, with barnacles embedded in fine-grained sediments displaying a better preservation of their C and O stable isotope signals than those embedded in coarse-grained and more permeable deposits. Barnacles are characterised by a complex structure that is perforated by structural cavities, like the parietal tubes, as well as by smaller-scale irregular voids in the microstructure, like those between the dragon scales and within the scales themselves (Fig. 13). Notwithstanding the low-magnesium calcite composition, these characteristics facilitate the alteration of the barnacle shells whenever contact with diagenetic fluids happens, thus suggesting that completely pristine preservation of the shell geochemical signature can commonly occur only when the shell is properly isolated from diagenetic and meteoric fluids. Since diagenesis causes modifications at the microscale that can only be detected with high resolution methodologies, a combination of screening procedures seems to be a requirement, starting with a careful sedimentological analysis of the matrix, down to SEM, CL and trace element investigations of the collected specimens.

Overall, in comparison to other groups of carbonate producers such as molluscs or corals, reference data on the composition of modern barnacle shells and its relationship with the surrounding environment are still largely wanting. The lack of extensive compilations on the composition of modern barnacle shells and reports on its intra-specimen variations have been also pointed out in the most recent reviews of the subject (Iglikowska et al., 2018; Ullmann et al., 2018). Significantly, even less is known about the stable isotope ratios of fossil barnacles, with only an handful of studies focusing on the strontium isotope ratio (e.g., Bosio et al., 2020; Paces et al., 2023), and four more focusing on the oxygen and carbon isotope ratios (Roskowski et al., 2010; Collareta et al., 2018; Taylor et al., 2019, 2022). This severely limits our ability of further interpreting our data without falling into speculation. However, our results indicate that, given an adequate diagenetic environment, fossil barnacles (including non-epizoic ones) can preserve a record of short-term (e.g., seasonal) environmental variations. Importantly, the specimens from Certaldo and Casenuove display no evidence of alteration, and their $\delta^{13}C$ and $\delta^{18}O$ values are reasonably consistent with those of their modern counterparts, indicating that the observed intra-shell variations are most likely related to short-term environmental changes. Further studies, focusing on fossil barnacles from fine-grained deposits, might be able to make up for the current lack of knowledge and release the untapped potential of barnacles for high-resolution, geochemically-based palaeoenvironmental analyses.

## 7. Conclusions

The analysis of several Western Mediterranean Pliocene and Pleistocene barnacle-rich deposits has provided an assessment of the (palaeo) environmental signal recorded by barnacle shells, as well as guidance on how to use them for palaeoenvironmental reconstructions. Within most barnacle-dominated carbonate systems, barnacle abundance is highest in shallow waters near the coast and decreases moving offshore, thus providing a good proxy for the reconstruction of water depth and distance from the coastline. This is consistent with other proxies such as the abundance of terrigenous particles, and the foraminiferal and coralline algal assemblages. Barnacle taphonomy is also highly informative: well-preserved complete specimens usually characterise protected settings, whereas poorly preserved, disarticulated and fragmented remains are generally dominant in exposed settings. The presence/absence of opercular plates is particularly relevant as these delicate elements are generally lost in high-energy settings. Some barnacles also display distinctive climatic preferences that can be used for palaeoenvironmental reconstruction; this is the case for *Concavus concavus*, whose distribution was essentially (sub)tropical.

Due to the coarse-grained nature of the deposits in which barnacle remains are usually found, a high level of scrutiny for diagenetic alteration must be applied when selecting specimens for geochemical analyses. Notwithstanding their stable, low-magnesium mineralogical composition and their apparent pristine state of preservation, most of the barnacle shells from coarse-grained deposits were found to be diagenetically altered, usually due to the interaction with meteoric waters. In turn, shells collected from fine-grained deposits displayed no major evidence of alteration in both SEM and cathodoluminescence analyses, and were characterised by C and O stable isotope ratios in line with those of their modern counterparts from the same geographical region (i.e., the Western Mediterranean). The best-preserved specimens also displayed intra-shell variations comparable to those observed in modern specimens and attributed to seasonal variations (or migration patterns in the case of epizoic barnacles). Unfortunately, the limited number of reports on such intra-specimen variability makes the interpretation of these data rather difficult.

Our results indicate that barnacles are useful palaeoenvironmental indicators and that their abundance in the skeletal assemblage can provide a wealth of useful information. Given a favorable

sedimentological context characterised by deposition of fine-grained sediments that shield shells from diagenesis, fossil barnacles might also be used for high-resolution geochemical analysis, thus providing data on short-term environmental variations.

## Declaration of Competing Interest

The authors declare that they have no known competing financial interests or personal relationships that could influence the work reported in this paper.

## Data availability

All the used data are in Supplementary table S1

## Acknowledgments

This paper was funded by a grant of the International Association of Sedimentologists (IAS Post-doctoral Grant Scheme, Spring 2020 edition) received by GC. All the authors are also grateful to the IAS for supporting their research activities and for creating an environment conducive to the development of this study. Additional funding that supported the detailed taxonomic analysis of barnacles was granted by the LinnéSys: Systematics Research Fund of the Linnean Society and the Systematics Association to GC and AC. The authors also acknowledge two anonymous reviewers whose comments significantly improved the paper and the Editorial Board of the journal for their help. The authors are also grateful to Stefano Zanchetta and Martina Rocca for their help and assistance with the cathodoluminescence analyses. Special thanks also go to the GAMPS (Gruppo Avis Mineralogia e Paleontologia Scandicci), and especially to Simone Casati, Andrea Di Cencio and Alice Pieri, for their help during field activities in the Pliocene-Pleistocene successions of Tuscany, as well as to Luca Mariani and Marco Merella, for their help with the laboratory activities.

## Appendix A. Supplementary data

Supplementary data to this article can be found online at https://doi.org/10.1016/j.palaeo.2023.111914.

## References

Achituv, Y., Brickner, I., Erez, J., 1997. Stable carbon isotope ratios in Red Sea barnacles (Cirripedia) as an indicator of their food source. Mar. Biol. 130, 243–247.
Adey, W.H., 1986. Coralline algae as indicators of sea-level. In: Van de Plassche, O. (Ed.), Sea-Level Research: A Manual for the Collection and Evaluation of Data. Geo-Books, Norwich, pp. 229–280.
Adey, W.H., Macintyre, I.G., 1973. Crustose coralline algae: a re-evaluation in the geological sciences. Geol. Soc. Am. Bull. 84, 883–904.
Ager, D.V., 1973. The Nature of the Stratigraphical Record. Wiley & Sons, Great Britain, p. 151.
Aguirre, J., Riding, R., Braga, J.C., 2000. Late Cretaceous incident light reduction: evidence from benthic algae. Lethaia 33 (3), 205–213.
Aguirre, J., Martín, J.M., Braga, J.C., Betzler, C., Berning, B., Buckeridge, J.S., 2008. Densely packed concentrations of sessile barnacles (Cirripedia: Sessilia) from the Early Pliocene of SE Spain. Facies 54 (2), 193–206.
Albuquerque, R., Queiroga, H., Swearer, S.E., Calado, R., Leandro, S.M., 2016. Harvest locations of goose barnacles can be successfully discriminated using trace elemental signatures. Sci. Rep. 6, 27787. https://doi.org/10.1038/srep27787.
Angiolini, L., Stephenson, M., Leng, M.J., Jadoul, F., Millward, D., Aldridge, A., Andrews, J., Chenery, S., Williams, G., 2012. Heterogeneity, cyclicity and diagenesis in a Mississippian brachiopod shell of palaeoequatorial Britain. Terra Nova 24 (1), 16–26.
Bailey, I., Hole, G.M., Foster, G.L., Wilson, P.A., Storey, C.D., Trueman, C.N., Raymo, M. E., 2013. An alternative suggestion for the Pliocene onset of major northern hemisphere glaciation based on the geochemical provenance of North Atlantic Ocean ice-rafted debris. Quat. Sci. Rev. 75, 181–194.
Barbin, V., 2000. Cathodoluminescence of carbonate shells: Biochemical vs diagenetic process. In: Pagel, M., Barbin, V., Blanc, P., Ohnenstetter, D. (Eds.), Cathodoluminescence in Geosciences. Springer Berlin Heidelberg, Berlin, Heidelberg, pp. 303–329.
Barbin, V., Gaspard, D., 1995. Cathodoluminescence of recent articulate brachiopod shells. Implications for growth stages and diagenesis evaluation. Geobios 28, 39–45.
Barnes, H., Klepal, W., Mitchell, B.D., 1976. The organic and inorganic composition of some cirripede shells. J. Exp. Mar. Biol. Ecol. 21 (2), 119–127.
Bartoli, G., Sarnthein, M., Weinelt, M., Erlenkeuser, H., Garbe-Schönberg, D., Lea, D.W., 2005. Final closure of Panama and the onset of northern hemisphere glaciation. Earth Planet. Sc. Lett. 237 (1–2), 33–44.
Basso, D., Nalin, R., Nelson, C.S., 2009. Shallow-water *Sporolithon* rhodoliths from North Island (New Zealand). Palaios 24, 92–103.
Beavington-Penney, S.J., Racey, A., 2004. Ecology of extant nummulitids and other larger benthic foraminifera: applications in palaeoenvironmental analysis. Earth Sci. Rev. 67 (3–4), 219–265.
Benvenuti, M., Bianchi, G., Bruttini, J., Buonicontri, M., Chiarantini, L., Dallai, L., Di Pasquale, G., Donati, A., Grassi, F., Pescini, V., 2014. Studying the Colline Metallifere mining area in Tuscany: an interdisciplinary approach. In: Proceedings of the Research and Preservation of Ancient Mining Areas, Yearbook of the Institute Europa Subterranea, 9th International Symposium on Archaeological Mining History. MuSe-Trento, Trento, pp. 5–8.
Bianucci, G., 1996. A new record of baleen whale from the Pliocene of Tuscany (Italy). Atti Soc. Tosc. Sci. Nat. Mem. Ser. A 102, 101–104.
Bianucci, G., Sorbini, C., 2014. Le collezioni a cetacei fossili del Museo di Storia Naturale dell'Università di Pisa. Museol. Sci. Mem. 13, 93–102.
Bianucci, G., Di Celma, C., Landini, W., Buckeridge, J., 2006. Palaeoecology and taphonomy of an extraordinary whale barnacle accumulation from the Plio-Pleistocene of Ecuador. Palaeogeogr. Palaeoclim. 24, 326–342.
Bigot-Cormier, F., Poupeau, G., Sosson, M., 2000. Dénudations différentielles du massif cristallin externe alpin de l'Argentera (Sud-Est de la France) révélées par thermochronologie trace de fission (apatites, zircons). C. R. Acad. Sci. Ser. IIA Earth Planet. Sci. 330 (5), 363–370.
Bizzarri, R., Baldanza, A., 2020. Integrated stratigraphy of the marine early Pleistocene in Umbria. Geosciences 10 (9), 371.
Bojar, A.V., Lécuyer, C., Bojar, H.P., Fourel, F., Vasile, Ş., 2018. Ecophysiology of the hydrothermal vent snail *Ifremeria nautilei* and barnacle *Eochionelasmus ohtai manusensis*, Manus Basin, Papua New Guinea: insights from shell mineralogy and stable isotope geochemistry. Deep-Sea Res. I Oceanogr. Res. Pap. 133, 49–58.
Boni, P., Peloso, G.F., Vercesi, P.L., 1976. I lembi pliocenici della Liguria Occidentale da San Lorenzo al Mare (Imperia) ad Andora (Savona). Atti Ist. Geol. Univ. Pavia 25, 112–142.
Borromeo, L., Zimmerman, U., Andò, S., Coletti, G., Bersani, D., Basso, D., Gentile, P., Schulz, B., Garzanti, E., 2017. Raman spectroscopy as a tool for magnesium estimation in Mg-calcite. J. Raman Spectrosc. 48 (7), 983–992.
Bosio, G., Malinverno, E., Collareta, A., Di Celma, C., Gioncada, A., Parente, M., Berra, F., Marx, F.G., Vertino, A., Urbina, M., Bianucci, G., 2020. Strontium isotope stratigraphy and the thermophilic fossil fauna from the middle Miocene of the East Pisco Basin (Peru). J. S. Am. Earth Sci. 97, 102399 https://doi.org/10.1016/j.jsames.2019.102399.
Bosio, G., Di Cencio, A., Coletti, G., Casati, S., Collareta, A., 2021. Exceptionally preserved coral bank and seagrass meadow from the Lower Pleistocene of Fauglia (Tuscany, Italy). Alp. Med. Quat. 34 (2), 237–256.
Bossio, A., Foresi, L.M., Liotta, D., Mazzanti, R., Mazzei, R., Salvatorini, G., Squarci, P., 1999. Riordino delle conoscenze sul Bacino neogenico del Tora-Fine (Toscana-Italia). Atti Soc. Tosc. Sci. Nat. Mem. Ser. A 106, 1–16.
Bourget, F., 1974. Environmental and structural control of trace elements in barnacle shells. Mar. Biol. 28 (1), 27–36.
Bourget, E., 1987. Barnacle shells: composition, structure and growth. Barnacle Biol. 5, 267–285.
Bourget, E., Crisp, D.J., 1975. An analysis of the growth bands and ridges of barnacle shell plates. J. Mar. Biol. Assoc. U. K. 55 (2), 439–461.
Breda, A., Mellere, D., Massari, F., 2007. Facies and processes in a Gilbert-delta-filled incised valley (Pliocene of Ventimiglia, NW Italy). Sediment. Geol. 200 (1–2), 31–55.
Breda, A., Mellere, D., Massari, F., Asioli, A., 2009. Vertically stacked Gilbert-type deltas of Ventimiglia (NW Italy): the Pliocene record of an overfilled Messinian incised valley. Sediment. Geol. 219 (1–4), 58–76.
Brogi, A., 2011. Bowl-shaped basin related to low-angle detachment during continental extension: the case of the controversial Neogene Siena Basin (Central Italy, Northern Apennines). Tectonophysics 499, 54–76.
Brogi, A., 2020. Late evolution of the inner Northern Apennines from the structure of the Monti del Chianti-Monte Cetona ridge (Tuscany, Italy). J. Struct. Geol. 141, 104205.
Brogi, A., Capezzuoli, E., Martini, I., Picozzi, M., Sandrelli, F., 2014. Late Quaternary tectonics in the inner Northern Apennines (Siena Basin, southern Tuscany, Italy) and their seismotectonic implication. J. Geodyn. 76, 25–45.
Buckeridge, J.S., 1975. Studies on the Non-pedunculate Lower Tertiary Cirripedia of New Zealand. Unpublished MSc thesis. University of Auckland, New Zealand, pp. 1–111.
Buckeridge, J.S., 1983. The fossil barnacles (Cirripedia: Thoracica) of New Zealand and Australia. New Zeal. Geol. Surv. Paleontol. Bull. 50, 1–51.
Buckeridge, J.S., 1999. A new deep sea barnacle, *Tetrachaelasma tasmanicum* sp. nov. (Cirripedia: Balanomorpha) from the South Tasman Rise, South Pacific Ocean. New Zeal. J. Mar. Fresh. 33 (4), 521–531. https://doi.org/10.1080/00288330.1999.9516897.
Buckeridge, J.S., 2015. Revision of Southern Hemisphere taxa referred to *Fosterella* Buckeridge, 1983 (Crustacea: Cirripedia), and their extinction in response to Pleistocene cooling. Integr. Zool. 10, 555–571. https://doi.org/10.1111/1749-4877.12161.
Buckeridge, J.S., Beu, A., Gordon, D., 2018a. Depositional environment of the early Pleistocene Castlepoint Formation, New Zealand: a canyon fill in situ. New Zeal. J. Geol. Geop. 61 (4), 524–542. https://doi.org/10.1080/00288306.2018.1516227.
Buckeridge, J.S., Chan, B.K., Lee, S.W., 2018b. Accumulations of fossils of the whale barnacle Coronula bifida Bronn, 1831 (Thoracica: Coronulidae) provides evidence of

a late Pliocene cetacean migration route through the Straits of Taiwan. Zool. Stud. 57.
Burgess, S.N., Henderson, G.M., Hall, B.L., 2010. Reconstructing Holocene conditions under the McMurdo Ice Shelf using Antarctic barnacle shells. Earth Planet. Sci. Lett. 298 (3–4), 385–393.
Cabioch, G., Montaggioni, L.F., Faure, G., Ribaud-Laurenti, A., 1999. Reef coralgal assemblages as recorders of paleobathymetry and sea level changes in the Indo-Pacific province. Quat. Sci. Rev. 18, 1681–1695.
Carminati, E., Wortel, M.J.R., Meijer, P.T., Sabadini, R., 1998. The two-stage opening of the western–Central Mediterranean basins: a forward modeling test to a new evolutionary model. Earth Planet. Sci. Lett. 160 (3–4), 667–679.
Carpenter, S.J., Lohmann, K.C., 1992. Sr/Mg ratios of modern marine calcite: empirical indicators of ocean chemistry and precipitation rate. Geochim. Cosmochim. Acta 56, 1837–1849.
Casella, L.A., Griesshaber, E., Roda, M.S., Ziegler, A., Mavromatis, V., Henkel, D., Laudien, J., Haussermann, V., Neuser, R.D., Angiolini, L., Dietzel, M., Eisenhauer, A., Immenhauser, A., Brand, U., Schmahl, W.W., 2018. Micro-and nanostructures reflect the degree of diagenetic alteration in modern and fossil brachiopod shell calcite: a multi-analytical screening approach (CL, FE-SEM, AFM, EBSD). Palaeogeogr. Palaeoclimatol. Palaeoecol. 502, 13–30.
Chave, K.E., 1954. Aspects of the biogeochemistry of magnesium 1. Calcareous marine organisms. J. Geol. 62 (3), 266–283.
Cheang, C.C., Tsang, L.M., Chu, K.H., Cheng, I.J., Chan, B.K., 2013. Host-specific phenotypic plasticity of the turtle barnacle *Chelonibia testudinaria*: a widespread generalist rather than a specialist. PLoS One 8 (3), e57592.
Christianen, M.J.A., Lengkeek, W., Bergsma, J.H., Coolen, J.W.P., Didderen, K., Dorenbosch, M., Driessen, F.M.F., Kamermans, P., Reuchlin-Hugenholtz, E., Sas, H., Smaal, A., van den Wijngaard, K.A., van der Have, T.M., 2018. Return of the native facilitated by the invasive? Population composition, substrate preferences and epibenthic species richness of a recently discovered shellfish reef with native European flat oysters (*Ostrea edulis*) in the North Sea. Mar. Biol. Res. 14 (6), 590–597.
Christie, A.O., Dalley, R., 1987. Barnacle fouling and its prevention. Barnacle Biol. 419–433.
Clarke, F.W., Wheeler, W.C., 1922. The inorganic constituents of marine invertebrates. US Government Printing Office, v. 124.
Coletti, G., Basso, D., 2020. Coralline algae as depth indicators in the Miocene carbonates of the Eratosthenes Seamount (ODP Leg 160, Hole 966F). Geobios 60, 29–46.
Coletti, G., Hrabovský, J., Basso, D., 2016. *Lithothamnion crispatum*: long-lasting species of non-geniculate coralline algae (Rhodophyta, Hapalidiales). Carnets Geol. 16 (03), 27.
Coletti, G., Basso, D., Corselli, C., 2018a. Coralline algae as depth indicators in the Sommières Basin (early Miocene, Southern France). Geobios 51 (1), 15–30.
Coletti, G., Bosio, G., Collareta, A., Buckeridge, J., Consani, S., El Kateb, A., 2018b. Palaeoenvironmental analysis of the Miocene barnacle facies: case studies from Europe and South America. Geol. Carpath. 69 (6), 573–592.
Coletti, G., Collareta, A., Bosio, G., Urbina-Schmitt, M., Buckeridge, J., 2019. *Perumegabalanus calziai* gen. et sp. nov., a new intertidal megabalanine barnacle from the early Miocene of Peru. Neues Jahrb. Geol. P.-A. 294, 197–212.
Coletti, G., Bosio, G., Collareta, A., 2021a. Lower Pliocene barnacle facies of western Liguria (NW Italy): a peek into a warm past and a glimpse of our incoming future. Riv. Ital. Paleontol. S. 127, 103–131.
Coletti, G., Mariani, L., Garzanti, E., Consani, S., Bosio, G., Vezzoli, G., Xiumian, H., Basso, D., 2021b. Skeletal assemblages and terrigenous input in the Eocene carbonate systems of the Nummulitic Limestone (NW Europe). Sediment. Geol. 425, 106005.
Collareta, A., 2020. Discovery of complemental males in a Pliocene accumulation of *Chelonibia testudinaria* (Linnaeus, 1758), with some notes on the evolution of androdioecy in turtle barnacles. Neues Jahrb. Geol. P.-A. 297 (2), 193–203.
Collareta, A., Bosselaers, M., Bianucci, G., 2016. Jumping from turtles to whales: a Pliocene fossil record depicts an ancient dispersal of *Chelonibia* on mysticetes. Riv. Ital. Paleontol. S. 122 (2), 35–44.
Collareta, A., Regattieri, E., Zanchetta, G., Lambert, O., Catanzariti, R., Bosselaers, M., Covelo, P., Varola, A., Bianucci, G., 2018. New insights on ancient cetacean movement patterns from oxygen-isotope analyses of a Mediterranean Pleistocene whale barnacle. Neues Jahrb. Geol. P.-A. 288, 143–159.
Collareta, A., Coletti, G., Bosio, G., Buckeridge, J., de Muizon, C., DeVries, T.J., Varas-Malca, R.M., Altamirano-Sierra, A., Urbina-Schmitt, M., Bianucci, G., 2019. A new barnacle (Cirripedia: Neobalanoformes) from the early Miocene of Peru: Palaeoecological and palaeobiogeographical implications. Neues Jahrb. Geol. P.-A. 292 (3), 321–338.
Collareta, A., Merella, M., Mollen, F.H., Casati, S., Di Cencio, A., 2020. The extinct catshark *Pachyscyllium distans* (Probst, 1879) (Elasmobranchii: Carcharhiniformes) in the Pliocene of the Mediterranean Sea. Neues Jahrb. Geol. P.-A. 295 (2), 129–139.
Collareta, A., Merella, M., Casati, S., Coletti, G., Di Cencio, A., 2021a. Another thermophilic“ Miocene survivor” from the Italian Pliocene: a geologically young occurrence of the pelagic eagle ray *Aetobatus* in the Euro-Mediterranean region. Carnets Geol. 21 (10), 203–214.
Collareta, A., Mollen, F.H., Merella, M., Casati, S., Di Cencio, A., 2021b. Remarkable multicuspid teeth in a new elusive skate (Chondrichthyes, Rajiformes) from the Mediterranean Pliocene. PalZ 95 (1), 117–128.
Collareta, A., Newman, W.A., Bosio, G., Coletti, G., 2022. A new chelonibiid from the Miocene of Zanzibar (Eastern Africa) sheds light on the evolution of shell architecture in turtle and whale barnacles (Cirripedia: Coronuloidea). Integr. Zool. 17 (1), 24–43.
Coutinho, L.M., Penelas Gomes, F., Nasri Sissini, M., Vieira-Pinto, T., de Oliveira, Muller, Henriques, M.C., Oliveira, M.C., Antunes Horta, P., de Barros, Barbosa, Barreto, M. B., 2022. Cryptic diversity in non-geniculate coralline algae: a new genus *Roseolithon* (Hapalidiales, Rhodophyta) and seven new species from the Western Atlantic. Eur. J. Phycol. 57 (2), 227–250.
Craven, K.F., Bird, M.I., Austin, W.E.N., Wynn, J., 2008. Isotopic variability in the intertidal acorn barnacle Semibalanus balanoides: a potentially novel sea-level proxy indicator. Geol. Soc. Lond. Spec. Publ. 303 (1), 173–185.
Crippa, G., Ye, F., Malinverno, C., Rizzi, A., 2016. Which is the best method to prepare invertebrate shells for SEM analysis? Testing different techniques on recent and fossil brachiopods. Boll. Soc. Paleontol. Ital. 55 (2), 112.
Crisp, D.J., Bourget, E., 1985. Growth in barnacles. Adv. Mar. Biol. 22, 199–244.
Crowley, T.J., Hyde, W., 2008. Transient nature of late Pleistocene climate variability. Nature 456 (7219), 226–230.
Dalla Giovanna, G., Fanucci, F., Pellegrini, L., Seno, S., Bonini, L., Decarlis, A., Maino, M., Morelli, D., Vercesi, P.L., Roccati, A., Cobianchi, M., Mancin, N., 2016. Note Illustrative Della Carta Geologica d'Italia Alla scala 1:50000, Foglio 259, Imperia. Servizio Geologico d'Italia, Roma.
Darmoian, S.A., Al-Marsoumi, A.H., 2002. Geochemistry of some carbonate secreting marine living organisms from the North West Arabian Gulf. Iraqi J. Earth Sci. 2, 1–14.
Davadie, C., 1963. Étude des balanes d'Europe et d'Afrique. Editions du Centre National de la Recherche Scientifique, Paris.
Detjen, M., Sterling, E., Gómez, A., 2015. Stable isotopes in barnacles as a tool to understand green sea turtle (*Chelonia mydas*) regional movement patterns. Biogeosciences 12 (23), 7081–7086.
Doglioni, C., Gueguen, E., Harabaglia, P., Mongelli, E., 1999. On the origin of West-directed subduction zones and applications to the Western Mediterranean. In: Durand, B., Jolivet, L., Horvath, E., Siranne, M. (Eds.), The Mediterranean Basins: Tertiary Extension within the Alpine Orogen, Geol. Soc. Lond. Spec. Publ, 156, pp. 541–561.
Dominici, S., Rook, L., Benvenuti, M., Abbazzi, L., 1995. Tapir remains in paralic depositsof Pliocene age in lower valdarno (Tuscany, Italy): Facies analysis and taphonomy. Geobios 28, 131–135.
Dominici, S., Danise, S., Benvenuti, M., 2018. Pliocene stratigraphic paleobiology in Tuscany and the fossil record of marine megafauna. Earth Sci. Rev. 176, 277–310.
Donovan, S.K., 1988. Palaeoecology and taphonomy of barnacles from the Plio-Pleistocene Red Crag of East Anglia. P. Geol. Assoc. 99 (4), 279–289.
Doyle, P., Mather, A.E., Bennet, M.R., Bussel, M.A., 1997. Miocene barnacle assemblages from Southern Spain and their palaeoenvironmental significance. Lethaia 29 (3), 267–274.
Dunham, R.J., 1962. Classification of carbonate rocks according to depositional texture. In: Ham, W.E. (Ed.), Classification of Carbonate Rocks, AAPG Bull, 1, pp. 108–121.
Embry, A.F., Klovan, J.E., 1971. A late Devonian reef tract on Northeastern Banks Island. NWT. B. Can. Petrol. Geol. 19, 730–781.
Epstein, S., Buchsbaum, R., Lowenstam, H.A., Urey, H.C., 1953. Revised carbonate-water isotopic temperature scale. Geol. Soc. Am. Bull. 64, 1315–1326.
Faccenna, C., Funiciello, F., Civetta, L., D'Antonio, M., Moroni, M., Piromallo, C., 2007. Slab disruption, mantle circulation, and the opening of the Tyrrhenian basins. In: Bianchini, G., Wilson, M. (Eds.), Beccaluva, L. Cenozoic Volcanism in the Mediterranean Area, Geological Society of America Special Paper, pp. 153–169. https://doi.org/10.1130/2007.2418(08).
Fanucci, F., Giammarino, S., Tedeschi, D., 1980. Il Pliocene della costa continentale dell'Appennino Ligure in rapporto alla neotettonica. Mem. Soc. Geol. Ital. 21, 259–265.
Flügel, E., 2010. Microfacies of Carbonate Rocks. Springer, Berlin, Heidelberg.
Foeken, J.P.T., Dunai, T.J., Bertotti, G., Andriessen, P.A.M., 2003. Late Miocene to present exhumation in the Ligurian Alps (southwest Alps) with evidence for accelerated denudation during the Messinian Salinity Crisis. Geology 31 (9), 797–800.
Gal, A., Weiner, S., Addadi, L., 2015. A perspective on underlying crystal growth mechanisms in biomineralisation: solution mediated growth versus nanosphere particle accretion. CrystEngComm 17, 2606.
Gale, A., Schweigert, G., 2016. A new phosphatic-shelled cirripede (Crustacea, Thoracica) from the Lower Jurassic (Toarcian) of Germany–the oldest epiplanktonic barnacle. Palaeontology 59 (1), 59–70.
Gelabert, B., Sàbat, F., Rodríguez-Perea, A., 2002. A new proposal for the late Cenozoic geodynamic evolution of the western Mediterranean. Terra Nova 14 (2), 93–100.
Giammarino, S., 1984. Evoluzione della Alpi Marittime liguri e sue relazioni con il Bacino Terziario del Piemonte ed il Mar Ligure. Atti Soc. Tosc. Sci. Nat. Mem. Ser. A. 91, 155–179.
Giammarino, S., Piazza, M., 2000. I conglomerati de Il Poggio (Imperia) nel quadro degli affioramenti pliocenici della Liguria occidentale. Atti Ticin. Sci. Terra 41, 33–39.
Giammarino, S., Fanucci, F., Orezzi, S., Rosti, D., Morelli, D., Cobianchi, M., Di Stefano, A., Fravega, P., Vannucci, G., Piazza, M., Finocchiaro, F., 2010. Note Illustrative Della Carta Geologica d'Italia Alla scala 1:50000, Foglio 258–271, San Remo. Servizio Geologico d'Italia, Roma.
Gordon, C.M., Carr, R.A., Larson, R.E., 1970. The influence of environmental factors on the sodium and manganese content of barnacle shells. Limnol. Oceanogr. 15 (3), 461–466.
Haven, D.S., Whitcomb, J.P., 1983. The origin and extent of oyster reefs in the James River, Virginia. J. Shellfish Res. 3 (2), 141.
Hayton, S., Nelson, C.S., Hood, S.D., 1995. A skeletal assemblage classification system for non-tropical carbonate deposits based on New Zealand Cenozoic limestones. Sediment. Geol. 100, 123–141.

Haywood, A.M., Hill, D.J., Dolan, A.M., Otto-Bliesner, B.L., Bragg, F., Chan, W.L., Chandler, M.A., Contoux, C., Dowsett, H.J., Jost, A., Kamae, Y., Lohmann, G., Lunt, D.J., Abe-Ouchi, A., Pickering, S.J., Ramstein, G., Rosenbloom, N.A., Salzmann, U., Sohl, L., Stepanek, C., Ueda, H., Yan, Q., Zhang, Z., 2013. Large-scale features of Pliocene climate: results from the Pliocene Model Intercomparison Project. Clim. Past 9 (1), 191–209.

Hill, D.J., Haywood, A.M., Lunt, D.J., Hunter, S.J., Bragg, F.J., Contoux, C., Stepanek, C., Sohl, L., Rosenbloom, N.A., Chan, W.L., Kamae, Y., Zhang, Z., Abe-Ouchi, A., Chandler, M.A., Jost, A., Lohmann, G., Otto-Bliesner, B.L., Ramstein, G., Ueda, H., 2014. Evaluating the dominant components of warming in Pliocene climate simulations. Clim. Past 10, 79–90. https://doi.org/10.5194/cp-10-79.

Hockett, D., Ingram, P., LeFurgey, A., 1997. Strontium and manganese uptake in the barnacle shell: electron probe microanalysis imaging to attain fine temporal resolution of biomineralization activity. Mar. Environ. Res. 43 (3), 131–143.

Hoskin, C.M., Reed, J.K., 1984. Barnacle plate sediment production by sheepshead, the Indian River, Florida. Geo-Marine Lett. 4 (1), 55–57.

Hover, V.C., Walter, L.M., Peacor, D.R., 2001. Early marine diagenesis of biogenic aragonite and Mg-calcite: new constraints from high-resolution STEM and AEM analyses of modern platform carbonates. Chem. Geol. 175 (3–4), 221–248.

Iglikowska, A., Ronowicz, M., Humphreys-Williams, E., Kukliński, P., 2018. Trace element accumulation in the shell of the Arctic cirriped Balanus balanus. Hydrobiologia 818, 43–56. https://doi.org/10.1007/s10750-018-3564-5.

Iryu, Y., 1992. Fossil non-articulated coralline algae as depth indicators for the Ryukyu Group. T. Proc. Palaeontol. Soc. Japan 167, 1165–1179.

Ivany, L.C., 2012. Reconstructing paleoseasonality from accretionary skeletal carbonates—challenges and opportunities. Paleontol. Soc. Papers 18, 133–166.

Khalifa, G.M., Weiner, S., Addadi, L., 2011. Mineral and matrix components of the operculum and shell of the barnacle *Balanus amphitrite*: calcite crystal growth in a hydrogel. Cryst. Growth Des. 11 (11), 5122–5130.

Killingley, J.S., 1980. Migrations of California gray whales tracked by oxygen-18 variations in their epizoic barnacles. Science 207 (4432), 759–760.

Killingley, J.S., Lutcavage, M., 1983. Loggerhead turtle movements reconstructed from $^{18}O$ and $^{13}C$ profiles from commensal barnacle shells. Estuar. Coast. Shelf S. 16 (3), 345–349.

Killingley, J.S., Newman, W.A., 1982. $^{18}O$ fractionation in barnacle calcite: a barnacle paleotemperature equation. J. Mar. Res. 40 (3), 893–902.

Klompmaker, A.A., Portell, R.W., Lad, S.E., Kowalewski, M., 2015. The fossil record of drilling predation on barnacles. Palaeogeogr. Palaeoclimatol. Palaeoecol. 426, 95–111.

Knauth, L.P., Kennedy, M.J., 2009. The late Precambrian greening of the Earth. Nature 460 (7256), 728–732.

Kregting, L.T., Hayden-Hughes, M., Millar, R.V., Joyce, P.W., Smyth, D.M., 2020. A first record of intertidal *Ostrea edulis* 3D structural matrices in Strangford Lough Northern Ireland-an emergent reef? J. Sea Res. 163, 101927.

Langer, M.R., Weinmann, A.E., Lötters, S., Rödder, D., 2012. "Strangers" in paradise: modeling the biogeographic range expansion of the foraminifera *Amphistegina* in the Mediterranean Sea. J. Foram. Res. 42 (3), 234–244.

Lees, A., Buller, A.T., 1972. Modern temperate-water and warm-water shelf carbonate sediments contrasted. Mar. Geol. 13 (5), M67–M73.

Lisiecki, L.E., Raymo, M.E., 2007. Plio–Pleistocene climate evolution: trends and transitions in glacial cycle dynamics. Quat. Sci. Rev. 26 (1–2), 56–69.

Lokier, S.W., Al Junaibi, M., 2016. The petrographic description of carbonate facies: are we all speaking the same language? Sedimentology 63, 1843–1885.

López, D.A., López, B.A., Arriagada, S.E., Mora, O.A., Bedecarratz, P.C., Pineda, M.O., González, M.L., Andrade, L.I., Uribe, J.M., Riquelme, V.A., 2012. Diversification of Chilean aquaculture: the case of the giant barnacle *Austromegabalanus psittacus* (Molina, 1782). Lat. Am. J. Aquat. Res. 40 (3), 596–607.

Loreto, M.F., Zitellini, N., Ranero, C.R., Palmiotto, C., Prada, M., 2021. Extensional tectonics during the Tyrrhenian back-arc basin formation and a new morpho-tectonic map. Basin Res. 33 (1), 138–158.

Lunt, D.J., Valdes, P.J., Haywood, A., Rutt, I.C., 2008. Closure of the Panama Seaway during the Pliocene: implications for climate and Northern Hemisphere glaciation. Clim. Dyn. 30 (1), 1–18.

Machel, H.G., 2000. Application of cathodoluminescence to carbonate diagenesis. In: Pagel, M., Barbin, V., Blanc, P., Ohnenstetter, D. (Eds.), Cathodoluminescence in Geosciences. Springer Berlin Heidelberg, Berlin, Heidelberg, pp. 271–301.

MacIntyre, I.G., Milliman, J.D., 1970. Physiographic features of the Outer Shelf and Upper Slope, Atlantic Continental Margin, Southeastern United States. Geol. Soc. Am. Bull. 81, 2577–2598.

Mariani, L., Coletti, G., Mateu-Vicens, G., Bosio, G., Collareta, A., Khokhlova, A., Di Cencio, A., Casati, S., Malinverno, E., 2022. Testing an indirect palaeo-seagrass indicator: Benthic foraminifera from the lower Pleistocene Posidonia meadow of Fauglia (Tuscany, Italy). Mar. Micropaleontol. 173, 102126.

Marroni, M., Mazzanti, R., Nencini, C., 1990. Geologia e geomorfologia delle Colline Pisane. Quad. Mus. St. Nat. Livorno 11 (1), 1–40.

Martini, I., Aldinucci, M., 2017. Sedimentation and basin-fill history of the Pliocene succession exposed in the northern Siena-Radicofani Basin (Tuscany, Italy): a sequence-stratigraphic approach. Riv. Ital. Paleontol. S. 123 (3), 407–432.

Martini, I.P., Sagri, M., 1993. Tectono-sedimentary characteristics of late Miocene-Quaternary extensional basins of the Northern Apennines, Italy. Earth-Sci. Rev. 34 (3), 197–233.

Martini, I., Ambrosetti, E., Brogi, A., Aldinucci, M., Zwaan, F., Sandrelli, F., 2021. Polyphase extensional basins: interplay between tectonics and sedimentation in the Neogene Siena-Radicofani Basin (Northern Apennines, Italy). Int. J. Earth Sci. 110 (5), 1729–1751.

Mateu-Vicens, G., Hallock, P., Brandano, M., Demchuk, T., Gary, A., 2009. Test shape variability of *Amphistegina* d'Orbigny 1826 as a paleobathymetric proxy: application to two Miocene examples. Geologic problems solving with microfossils. SEPM Spec. Publ. 93, 67–82.

Mazzanti, R., 2016. Note Illustrative Della Carta Geologica d'Italia Alla scala 1:50.000, Foglio 284, Rosignano Marittimo. Servizio Geologico d'Italia, ISPRA, Roma, p. 189.

Menesini, E., 1965. Caratteri morfologici e struttura microscopica di alcune specie di balani neogenici. Paleontographia Italica 59, 85–129.

Merella, M., Collareta, A., Casati, S., Di Cencio, A., Bianucci, G., 2023. Pliocene Geotourism: innovative projects for valorizing the paleontological heritage of three different-staged quarries of Tuscany (central Italy). Geoheritage 15, 82.

Michel, J., Mateu-Vicens, G., Westphal, H., 2011. Modern Heterozoan carbonates from a eutrophic tropical shelf (Mauritania). J. Sediment. Res. 81 (9), 641–655.

Milliman, J.D., 1972. Atlantic Continental Shelf and Slope of the United States-Petrology of the Sand Fraction of Sediments, Northern New Jersey to Southern Florida. US Geol. Surv. Prof. Pap. 529-J, 1–48.

Minnery, G.A., Rezak, R., Bright, T.J., 1985. Depth zonation and growth form of crustose coralline algae: Flower Garden Banks, Northwestern Gulf of Mexico. In: Toomey, D. F., Nitecki, M.H. (Eds.), Paleoalgology: Contemporary Research and Applications. Springer, New York, pp. 237–246.

Nalin, R., Ghinassi, M., Basso, D., 2010. Onset of temperate carbonate sedimentation during transgression in a low-energy siliciclastic embayment (Pliocene of the Val d'Orcia Basin, Tuscany, Italy). Facies 56, 353–368.

Nalin, R., Ghinassi, M., Foresi, L.M., Dallanave, E., 2016. Carbonate deposition in restricted basins: a Pliocene case study from the Central Mediterranean (Northwestern Apennines), Italy. J. Sediment. Res. 86 (3), 236–267.

Newman, W.A., 1982. A review of extant taxa of the "group of *Balanus concavus*" (Cirripedia, Thoracica) and a proposal for genus-group ranks. Crustaceana 43 (1), 25–36.

Newman, W.A., Killingley, J.S., 1985. The north-east Pacific intertidal barnacle *Pollicipes polymerus* in India? A biogeographical enigma elucidated by $^{18}O$ fractionation in barnacle calcite. J. Nat. Hist. 19 (6), 1191–1196.

Newman, W.A., Zullo, V.A., Wainwright, S.A., 1967. A critique on recent concepts of growth in Balanomorpha (Cirripedia, Thoracica). Crustaceana 12 (2), 167–178.

Nielsen, J.K., Funder, S., 2003. Taphonomy of Eemian marine molluscs and acorn barnacles from eastern Arkhangelsk region, northern Russia. Palaeogeogr. Palaeocl. 191 (2), 139–168.

Nomura, S., Maeda, H., 2008. Significance of autochtonous fossil barnacles from the Miocene Natori Group at the Moniwa-Goishi area, Northeast Japan. Paleontol. Res. 12 (1), 63–79.

Paces, J.B., Minor, S.A., Schmidt, K.M., Hoffman, J., 2023. Strontium isotope chronostratigraphic age of a sirenian fossil site on Santa Rosa Island, Channel Islands National Park, California (No. 2023-5026). US Geological Survey.

Patacci, M., 2016. A high-precision Jacob's staff with improved spatial accuracy and laser sighting capability. Sediment. Geol. 335, 66–69.

Pearson, R.M., van de Merwe, J.P., Gagan, M.K., Limpus, C.J., Connolly, R.M., 2019. Distinguishing between sea turtle foraging areas using stable isotopes from commensal barnacle shells. Sci. Rep. 9 (1), 6565.

Pearson, R.M., van de Merwe, J.P., Connolly, R.M., 2020. Global oxygen isoscapes for barnacle shells: Application for tracing movement in oceans. Sci. Total Environ. 705, 135782.

Pilkey, O.H., Harris, R.C., 1966. The effect of intertidal environment on the composition of calcareous skeletal material 1. Limnol. Oceanogr. 11 (3), 381–385.

Pitombo, F.B., 2004. Phylogenetic analysis of the Balanidae (Cirripedia, Balanomorpha). Zool. Scr. 33 (3), 261–276.

Plancq, J., Grossi, V., Pittet, B., Huguet, C., Rosell-Melé, A., Mattioli, E., 2015. Multi-proxy constraints on sapropel formation during the late Pliocene of central Mediterranean (southwest Sicily). Earth Planet. Sci. Lett. 420, 30–44.

Prista, G.A., Agostinho, R.J., Cachão, M.A., 2015. Observing the past to better understand the future: a synthesis of the Neogene climate in Europe and its perspectives on present climate change. Open Geosci. 7 (1), 20150007.

Radwańska, U., Radwański, A., 2008. Eco-taphonomy of mass-aggregated giant balanids *Concavus (Concavus) concavus* (Darwin, 1854) from the Lower Pliocene (Zanclean) of Rafina near Pikermi (Attica, Greece). Acta Geol. Pol. 58 (1), 87–03.

Railsback, L.B., Anderson, T.F., Ackerly, S.C., Cisne, J.L., 1989. Paleoceanic modeling of temperature-salinity profiles from stable isotope data. Paleoceanogr. 4, 585–591.

Raymo, M.E., Oppo, D.W., Curry, W., 1997. The mid-Pleistocene climate transition: a deep sea carbon isotopic perspective. Paleoceanogr. 12 (4), 546–559.

Rehault, J.P., Boillot, G., Mauffret, A., 1984. The Western Mediterranean Basin geological evolution. Mar. Geol. 55 (3–4), 447–477.

Rehault, J.P., Boillot, G., Mauffret, A., 1985. The Western Mediterranean Basin. In: Stanley, D.J., Wezel, F.-C. (Eds.), Geological Evolution of the Mediterranean Basin. Springer, New York, pp. 101–129.

Reijmer, J.J.G., Bauch, T., Schäfer, P., 2012. Carbonate facies patterns in surface sediments of upwelling and non-upwelling shelf environments (Panama, East Pacific). Sedimentology 59 (1), 32–56.

Reis, P.A., Salgado, M.A., Vasconcelos, V., 2011. Barnacles as biomonitors of metal contamination in coastal waters. Estuar. Coast. Shelf Sci. 93 (4), 269–278.

Reymond, C.E., Zihrul, K.S., Halfar, J., Riegl, B., Humphreys, A., Hildegard, W., 2016. Heterozoan carbonates from the equatorial rocky reefs of the Galapagos Archipelago. Sedimentology 63 (4), 940–958.

Reynaud, J.Y., James, N.P., 2012. The Miocene Sommières basin, SE France: Bioclastic carbonates in a tide-dominated depositional system. Sediment. Geol. 282, 360–373.

Roskowski, J.A., Patchett, P.J., Spencer, J.E., Pearthree, P.A., Dettman, D.L., Faulds, J.E., Reynolds, A.C., 2010. A late Miocene–early Pliocene chain of lakes fed by the Colorado River: evidence from Sr, C, and O isotopes of the Bouse Formation and

related units between Grand Canyon and the Gulf of California. Bulletin 122 (9–10), 1625–1636.
Rustioni, M., Mazza, P., 2001. Taphonomic analysis of *Tapirus arvernensis* remains from the lower Valdarno (Tuscany, Central Italy). Geobios 34 (4), 469–474.
Sanfilippo, R., Kočí, T., Bosio, G., Collareta, A., Ekrt, B., Malinverno, E., Di Celma, C., Urbina, M., Bianucci, G., 2021. An investigation of vermetid reefs from the Miocene of Peru, with the description of a new species. J. S. Am. Earth Sci. 108, 103233.
Sanford, E., Menge, B.A., 2001. Spatial and temporal variation in barnacle growth in coastal upwelling system. Mar. Ecol. Prog. Ser. 209, 143–157.
Savelli, C., 2015. Fast episodes of West-Mediterranean-Tyrrhenian oceanic opening and revisited relations with tectonic setting. Sci. Rep. 5 (1), 14271.
Seilacher, A., 2005. Whale barnacles: exaptational access to a forbidden paradise. Paleobiology 31 (2), 27–35.
Shackleton, N.J., 1987. Oxygen isotopes, ice volume and sea level. Quat. Sci. Rev. 6 (3–4), 183–190.
Shackleton, N.J., Backman, J., Zimmerman, H., Kent, D.V., Hall, M.A., Roberts, D.G., Schnitker, D., Baldauf, J.G., Desprairies, A., Hominghausen, R., Huddlestun, P., Keene, J.B., Kaltenback, A.J., Krumsiek, K.A.O., Morton, A.C., Murray, J.W., Westberg-Smith, J., 1984. Oxygen isotope calibration of the onset of ice-rafting and history of glaciation in the North Atlantic region. Nature 307 (5952), 620–623.
Sharp, Z., 2017. Principles of stable isotope geochemistry. https://doi.org/10.25844/h9q1-0p82.
Símonarson, L.A., 1981. Cerastoderma edule (Linné, 1767) and its migration to Iceland. Arct. Alp. Res. 13 (1), 105–112.
Smith, H.S., Delafontaine, M., Flemming, B.W., 1988. Intertidal barnacles—Assessment of their use as paleo-environment indicators using Mg, Sr, $^{18}O/^{16}O$ and $^{13}C/^{12}C$ variations. Chem. Geol. 73 (3), 211–220.
Swain, G.W., Nelson, W.G., Preedeekanit, S., 1998. The influence of biofouling adhesion and biotic disturbance on the development of fouling communities on non-toxic surfaces. Biofouling 12 (1–3), 257–269.
Taylor, L.D., O'Dea, A., Bralower, T.J., Finnegan, S., 2019. Isotopes from fossil coronulid barnacle shells record evidence of migration in multiple Pleistocene whale populations. P. Natl. A. Sci. USA 116 (15), 7377–7381.
Taylor, L.D., Abella, J., Morales-Saldaña, J.M., 2022. New fossil remains of the commensal barnacle Cryptolepas rhachianecti provide evidence of gray whales in the prehistoric South Pacific. J. Paleontol. 96 (3), 583–590.
Triantaphyllou, M.V., Koukousioura, O., Dimiza, M.D., 2009. The presence of the Indo-Pacific symbiont-bearing foraminifer *Amphistegina lobifera* in Greek coastal ecosystems (Aegean Sea, Eastern Mediterranean). Mediterr. Mar. Sci. 10 (2), 73–86.
Türkmen, M., Türkmen, A., Akyurt, I., Tepe, Y., 2005. Limpet, *Patella caerulea* Linnaeus, 1758 and barnacle, *Balanus* sp., as biomonitors of trace metal availabilities in Iskenderun Bay, northern east Mediterranean sea. B. Environ. Contam. Tox. 74 (2), 301–307.
Ullmann, C.V., Gale, A.S., Huggett, J., Wray, D., Frei, R., Korte, C., Broom-Fendley, S., Littler, K., Hesselbo, S.P., 2018. The geochemistry of modern calcareous barnacle shells and applications for palaeoenvironmental studies. Geochim. Cosmochim. Acta 243, 149–168.
Van Dijk, J.P., Scheepers, P.J.J., 1995. Neotectonic rotations in the Calabrian Arc; implications for a Pliocene-recent geodynamic scenario for the Central Mediterranean. Earth Sci. Rev. 39 (3–4), 207–246.
Violanti, D., 2012. Pliocene Mediterranean foraminiferal biostratigraphy: A synthesis and application to the paleoenvironmental evolution of Northwestern Italy. In: Elitok, Ö. (Ed.), Stratigraphic Analysis of Layered Deposits. Intech Open, London, pp. 123–160.
Walker, G., Foster, P., 1979. Seasonal variation of zinc in the barnacle, *Balanus balanoides* (L.) maintained on a raft in the Menai Strait. Mar. Environ. Res. 2 (3), 209–221.
Watson, D., Foster, P., Walker, G., 1995. Barnacle shells as biomonitoring material. Mar. Pollut. Bull. 31 (1–3), 111–115.
Zardus, J.D., Lake, D.T., Frick, M.G., Rawson, P.D., 2014. Deconstructing an assemblage of "turtle" barnacles: species assignments and fickle fidelity in *Chelonibia*. Mar. Biol. 161, 45–59.
Zullo, V.A., 1992. Revision of the balanid barnacle genus *Concavus* Newman, 1982, with the description of a new subfamily, two new genera, and eight new species. Paleontol. Soc. Memoir 27, 1–46.